




KS5 Pilot Plant Study Report

Pilot Plant test report

<i>Document Number</i>	G4-V30902-0002	
<i>Version</i>	0	
<i>Submitted By</i>	Tom Dufty 	
<i>Reviewed By:</i>	Matthew Gill 	
<i>Document Approved:</i>	Matthew Gill 	
<i>Date Approved</i>	01/11/2023	
<i>Document Distribution Approval:</i>	<input type="checkbox"/> Internal Only <input checked="" type="checkbox"/> External	<input type="checkbox"/> Confidential <input checked="" type="checkbox"/> Public
<i>Document Type</i>	Pilot Plant Test report	
<i>Managed By</i>	Engineering	

<i>Rev</i>	<i>Prepared</i>	<i>Review</i>	<i>Approved</i>	<i>Date</i>	<i>Reason For Revision</i>
0	TD,YX,JF,PS,SS	MG,MBH,GB	MG MG	01/11/23	For Issue to Arena

All intellectual property rights contained in this document are owned by Calix Limited. The information contained in this document is confidential to Calix Limited. Access to this document and the information contained in this document by any party or person without the consent of Calix Limited is unauthorised. If you are not the authorised recipient, any use, disclosure, copying, or distribution of this document, or any action taken or omitted to be taken in reliance on it, is prohibited and may be unlawful.

CONTENTS

1	Executive Summary.....	9
2	Project Overview and Pilot Plant Study Objectives	10
2.1	Scope.....	10
2.1.1	BATMn Pilot Plant Setup for the ZESTY Campaign.....	11
3	General Results	13
3.1	ZESTY Experimental Test Program	13
3.2	Materials and Methodology	14
3.2.1	Materials	14
3.2.2	Methodology.....	19
3.2.3	Material Recovery Calculation	21
3.3	Campaign Results for Goethite and Hematite Blend G01 and G05 Ores.....	22
3.3.1	The Effect of Temperature on Reduction Degree and Collection Efficiency	22
4	Briquetting and Smelting Trials Update.....	34
4.1	Hot Briquetted Iron (HBI).....	34
4.1.1	Hot Briquetted Iron (HBI) test work plan.....	35
4.1.2	Direct Reduced Iron (DRI) – sample transport and testing update	35
5	Competitive Technologies Assessment.....	36
5.1	Introduction	36
5.2	Zero Emissions Steel Technology (ZESTY)	37
5.3	Description of the Competitive Technologies.....	38
5.3.1	Flash Ironmaking Technology (FIT)	38
5.3.2	Pilot Plant Flash Reactor	40
5.3.3	Medium Sized Flash Ironmaking Reactors	41
5.3.4	Design of Industrial Flash Ironmaking Reactors.....	42
5.4	Fluidised Bed Processes	43
5.4.1	FINMET.....	43
5.4.2	Circored.....	43
5.4.3	Hismelt.....	45
5.4.4	HYFOR – Hydrogen-based Fine-Ore Reduction.....	46
5.4.5	Hydrogen reduction – HyREX.....	47

5.5	Comparison Between The Technologies.....	49
5.5.1	Characteristics of The Process	49
5.5.2	Techno-economic Comparison	51
5.5.3	Technological Readiness Level.....	52
6	Emissions Reduction Potential.....	53
7	Site Selection Conclusions.....	55
7.1	Site Selection Executive Summary	56
7.2	Technology and Types of Electrolysers Summary:.....	58
8	Conclusions and Next Steps	61
9	References	62

FIGURES

Figure 1 A simplified schematic of Calix’s Zero Emission Steel Technology (ZESTY).	11
Figure 2 Process flow for 30kTpa ZESTY green steel production.....	12
Figure 3 X-ray diffractogram of the goethite and hematite blend G01 assessed for initial benchmarking.	15
Figure 4 X-ray diffractogram of the goethite and hematite blend G05.....	16
Figure 5 Particle size distributions (PSD) of the goethite and hematite blend G01 ore of different particle sizes using laser diffraction technique.	17
Figure 6 PSD of the goethite and hematite blend G0503 ore using laser diffraction technique.	18
Figure 7 TGA-H ₂ reduction extent measurement profile	20
Figure 8 Reduction degree and material collection efficiency tested with various temperatures for the G01 ores FeO-0114 at an H ₂ ratio of 2:1 and a 1 kg/min feed rate.....	22
Figure 9 Metallisation degree tested with various temperatures for the G01 ores FeO-0114 and G0109, at an H ₂ ratio of 2:1 and a 1 kg/min feed rate.....	22
Figure 10 Reduction and material recovery tested with G0503 at 950°C, H ₂ /Ored ratio of 2:1, feed rate of 1 kg/min.	23
Figure 11 PSD results of samples from G0114 reduced at various temperatures with an H ₂ ratio of 2:1 and a 1 kg/min feed rate.	23
Figure 12 Clumps were formed in the processed G0114 DRI at 1050°C.	24
Figure 13 PSD measurements of the ores employed in the 2023 ZESTY campaign compared to the goethite/hematite HG57 ore used during the 2022 proof-of-concept campaign.	25
Figure 14 Metallisation degree as a function of wall temperature setpoint. (Ore type = various; T _{wall} = variable; Feed rate = 1 kg/min; H ₂ stoichiometric ratio = 2 for ores a-f and 1.5:1 for g)	25
Figure 15 Reduction degree of reduced products as a function of wall temperature setpoint. (Ore type = various; T _{wall} = variable; Feed rate = 1 kg/min; H ₂ stoichiometric ratio = 2 for ores a-f and 1.5:1 for g).	26
Figure 16 Reduction, metallisation, and material recovery tested with various particle sizes at 950°C, H ₂ /Ored ratio of 2:1, feed rate of 1 kg/min.	26
Figure 17 PSD comparison of raw, bulk, baghouse, and cyclone samples from G0109 reduced at 1000°C, H ₂ /Ored ratio of 2:1 and feed rate of 1 kg/min.	27
Figure 18 PSD comparison of the raw, bulk sample and off-gas sample from the G0114 ore.....	28
Figure 19 a) Reduction and material recovery b) metallisation and material recovery tested with various H ₂ ratio for the ore G0114, at 1000C and feed rate of 1.6 kg/min.....	29
Figure 20 PSD results from various H ₂ ratio (labelled in figure) for the ore G0114, at 1000C and feed rate of 1.6 kg/min.	29
Figure 21 Specific Surface area of DRI samples generated from various feed rates for the ore G0114, at 1000 °C, H ₂ ratio of 2:1.	30
Figure 22 Material recovery performance under various feed rates under different H ₂ flow rates for the ore G0114, at 1000°C, H ₂ ratio of 2:1.....	30
Figure 23 Material recovery tested with various feed rates for the ore G0114, at H ₂ /Ored ratio at 1000°C.	31
Figure 24 . a) Material reduction degree b) metallisation degree tested with various feed rates for the ore G0114, at H ₂ /Ored ratio at 1000°C.....	31

Figure 25 Reduction degree tested with various H ₂ /Ored ratios at 1kg/min feed rates and 1.6kg/min for the ore G0114, at 1000°C.	32
Figure 26 Material recovery tested with various H ₂ /Ored ratios at 1kg/min feed rates and 1.6kg/min for the ore G0114, at 1000°C.	32
Figure 27 PSD comparisons between the unprocessed 0503 ore and the DRI samples produced from the G0503 ore under various trial conditions.	33
Figure 28 Schematic of the ZESTY reactor (1)	37
Figure 29 A schematic diagram of flash ironmaking and a possible direct steelmaking process (8) (9)	39
Figure 30 Laboratory flash reactor (7) (8)	40
Figure 31 Pilot plant flash reactor (8)	41
Figure 32 Different configuration of FIT reactor (8)	42
Figure 33 FINMET Process (10) (12)	44
Figure 34 Circored Process (10) (13)	44
Figure 35 FINEX Process (10) (14)	45
Figure 36 Hismelt process (10) (16)	45
Figure 37 HYFOR Pilot plant (17)	46
Figure 38 HYFOR Industrial prototype plant (17)	47
Figure 39 HyREX process flowsheet (18)	48

TABLES

Table 1 ZESTY campaign test matrix for goethite/hematite ores.....	13
Table 2 Phase 1 test plan for G05 goethite and hematite blend ore.....	13
Table 3 Dominant mineral compositions of the goethite and hematite blend G01 ore used in the initial goethite and hematite blend ore benchmarking test and the G05 ore.....	15
Table 4 Mineralogical composition of goethite and hematite blend G01 and G05 ore by quantitative XRD.....	17
Table 5 PSD summary of the goethite and hematite blend G01 ore of different particle sizes and the G0503 ore using laser diffraction technique.....	18
Table 6 Specific surface area (SSA) and pore properties of the goethite and hematite blend G01 ores of different targeted particle size distributions assessed for initial benchmarking and the G0503 ore.....	18
Table 7 Specifications of the milled G01 goethite and hematite blended ore milled to a target particle size specification of (d80 = 100 µm and 200 µm).....	24
Table 8 PSD and reduction degree of raw, bulk, baghouse, and cyclone samples from G0109 reduced at 1000°C, H ₂ /Ored ratio of 2:1 and feed rate of 1 kg/min.....	27
Table 9 Industrial Flash Ironmaking Reactors (8).....	42
Table 10 Gas composition and metallization rate at the reactor outlets (8).....	43
Table 11 Comparison between the technologies based on characteristics of the process.....	49
Table 12 Comparison between the technologies based on techno-economics of the process.....	51
Table 13 Comparison between the technologies based on TRL level.....	52
Table 14 Comparison between the technologies based on CO ₂ emission.....	54
Table 15 Comparison between the technologies based on CO ₂ reduction potential.....	54
Table 16 Comparative Table of Advantages and Disadvantages.....	58

DEFINITIONS

BoD	-	Basis of Design
BF	-	Blast Furnace
BOF	-	Basic Oxygen Furnace
Calciner	-	Calix Flash Calciner Reactor, or CFC Reactor
CAPEX	-	Capital Expenditure
CCUS	-	Carbon Capture Utilisation and Storage
CFC	-	Calix Flash Calciner
CO	-	Carbon Monoxide
CO ₂	-	Carbon Dioxide
DR	-	Direct Reduction
DRI	-	Direct Reduced Iron
EAF	-	Electric Arc Furnace
e-CFC	-	Electric Calix Flash Calciner
EPCM	-	Engineering, Procurement, and Construction Management
FEED	-	Front-End Engineering Design
H ₂	-	Hydrogen
H ₂ O	-	Steam or Water
H-DRI	-	Hydrogen DRI
HBI	-	Hot Briquetted Iron
HHBI	-	Hydrogen HBI
HX	-	Heat Exchanger
HYBRIT	-	Hydrogen Breakthrough Ironmaking Technology
LEILAC™	-	Low Emissions Lime and Cement
MEL	-	Mechanical Equipment List
MOU	-	Memorandum of Understanding
MS	-	Milestone
OPEX	-	Operational Expenditure
Pre-FEED	-	Preliminary Front-End Engineering Design
PDC	-	Process Design Criteria
LKAB	-	Luossavaara-Kiirunavaara Aktiebolag
IEA	-	International Energy Agency
PSD	-	Particle Size Distribution
SAF	-	Submerged Arc Furnace
SSAB	-	Svenskt Stål AB
tls	-	Tonnes of Liquid Steel
TPD	-	Tonnes Per Day
TPA	-	Tonnes Per Annum
ZESTY	-	Zero Emissions Steel Technology

DISCLAIMER

This report has been prepared for Formal Company Name (Common Company Name) by Calix Ltd (Calix) as an independent consultant and is based in part on information furnished by Common Company Name and in part on information not within the control of either Common Company Name or Calix. While it is believed that the information, conclusions and recommendations will be reliable under the conditions and subject to the limitations set forward herein, Calix does not guarantee their accuracy. The use of this report and the information contained herein shall be at the user's sole risk, regardless of any fault or negligence of Calix.

This project received funding from the Australian Renewable Energy Agency (ARENA) as part of ARENA's Advancing Renewables Program.

The views expressed herein are not necessarily the views of the Australian Government. The Australian Government does not accept responsibility for any information or advice contained within this document.

Parts of this report have been completed through engagement of Swinburn University of Technology and leverages prior work done in conjunction with the HILT CRC.

1 EXECUTIVE SUMMARY

The pilot plant test work has been completed at Calix's Bacchus Marsh R&D facility.

The pilot plant test results showed good metallisation rates across a range of process conditions with some clear identifiable trends that allow for further development of reactor models and optimisation of process parameters for the pilot plant.

The upgrades to the plant have proven successful in returning elutriated powder back into the reactor, with collection efficiencies significantly increased over the initial proof of concept trials run in 2022. Certain process conditions however did demonstrate reduced collection efficiencies. Additional work is being undertaken to further understand the retention of material in the system and test mitigation measures.

Progress has been made towards assessing the downstream processing of ZESTYDRI with initial trials being conducted at Swinburne University of Technology (SUT) and samples being sent to Köppern in Germany for briquetting test work.

Site selection work has been progressed further into specific site details, with the ultimate decision to be driven by commercial arrangements with upstream or downstream partners. From a technical and techno-economic perspective, sites in South Australia offer several advantages with regard to access to utilities and ability to use a higher proportion of green electricity.

Emissions reduction and techno-economics have been developed further towards completion of the FEED study. This milestone report includes summaries of comparisons between ZESTY and other technologies.

2 PROJECT OVERVIEW AND PILOT PLANT STUDY OBJECTIVES

2.1 Scope

The ZESTY ARENA project is structured around distinct engineering and development phases and milestones to ensure that the project proceeds with the endorsement and support of Australian iron ore and steel producers for a demonstration plant. Calix has completed a pre-FEED study with a FEED study underway for a 30,000 TPA H-DRI commercial demonstration plant using Calix's ZESTY process. To inform the FEED study, upgrades to the pilot plant and a series of pilot test work has been completed.

The pilot plant study has multiple objectives to allow for the further understanding of the performance and flexibility of the ZESTY process.

Primarily the goals are:

- Understand operating windows of the pilot plant and how the following process parameters effect the performance of the process:
 - Particle size
 - Operating temperature
 - Hydrogen excess flow ratio (ratio of H₂ to stoichiometric value)
- Understand the differences in performance between differing ore compositions to understand market position and economics.
- Develop Calix's internal process and operating expertise around handling Hydrogen and DRI.

2.1.1 BATMn Pilot Plant Setup for the ZESTY Campaign

The pilot plant, as shown in Figure 1, features a vertical reactor tube with an internal diameter of 0.2 m and a heated length of 18 m consisting of 18 independently controlled electric furnace zones. This setup enables precise control of the wall and process temperatures from ambient up to >1000 °C. Iron ore fines are introduced through the top of the reactor via a screw feeder operating in a semi-continuous mode at a feed rate of up to 150 kg/h. In counter-flow, hydrogen gas (H₂) is supplied from the reactor's base, with stoichiometric ratios ranging from 1.2 to 2. Direct Reduced Iron (DRI) products are collected in sealed collection vessels connected at the base of the reactor. The section of the reactor tube between the heated section and the collection vessel at the base of the reactor is water cooled to quench the product temperature and arrest further reduction of the product in the collection vessel. The product collection vessel is purged with a low flow of argon, as an additional measure to quench the reaction and protect the integrity of the product.

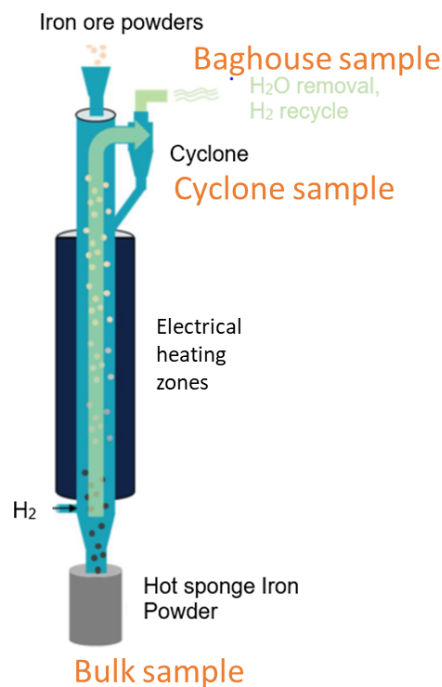


Figure 1 A simplified schematic of Calix's Zero Emission Steel Technology (ZESTY).

The proposed scaled-up commercial demonstration plant, as depicted in Figure 2, outlines an integrated system targeting an annual production capacity of 30,000 metric tonne of DRI. The electric ZESTY reactor (3) will be responsible for the calcination and reduction processes, which can be powered by sustainably produced renewable energy. The plant will also feature a heat recovery steam generator (4), which captures hot exhaust gas from the ZESTY reactor. This recovered heat will be utilised to drive a steam turbine (4) to generate supplemental electricity for the plant.

The electricity generated is earmarked for an electrolyser unit (5), which will subsequently produce hydrogen (H₂) and oxygen (O₂). The H₂ is cycled back into the ZESTY reactor and serves as a reducing

agent for iron. Concurrently, the generated oxygen could be routed to a melter, where it combines with the DRI product from the ZESTY reactor (3). This integrated circular approach will help to complete the production of green steel, thereby aligning with the broader goals of industrial sustainability and reduced carbon footprint.

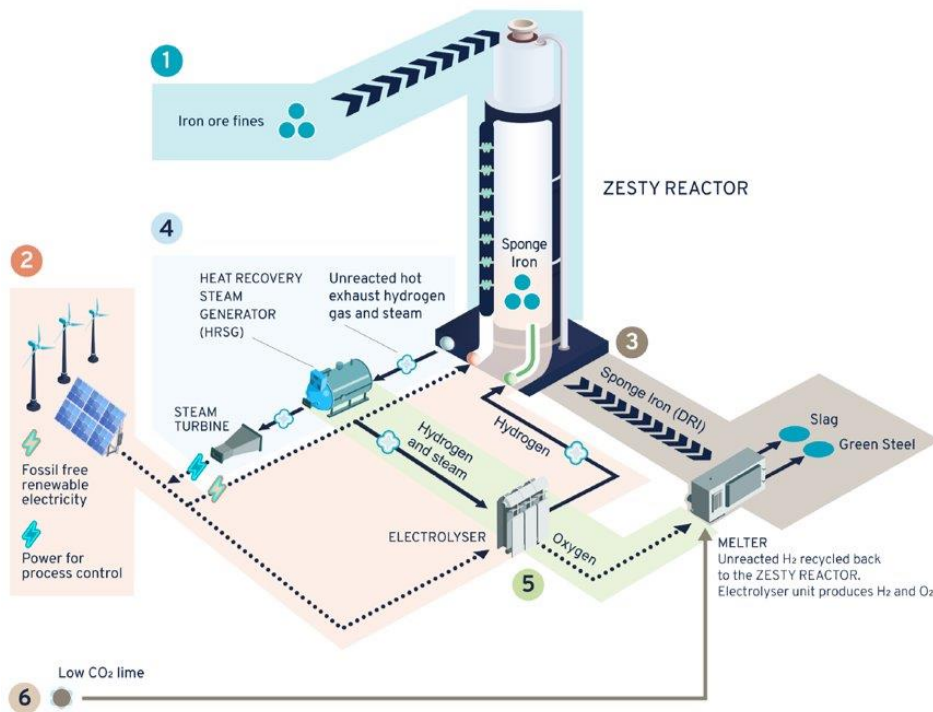


Figure 2 Process flow for 30kTpa ZESTY green steel production

3 GENERAL RESULTS

3.1 ZESTY Experimental Test Program

The ZESTY program has commenced with an initial benchmarking exercise, using goethite/hematite and magnetite ores to assess the effect of key processing parameters such as temperature, PSD, hydrogen ratio, and feed rate on key performance metrics including (but not limited to) metallisation extent and product collection efficiency. This pilot plant report will focus on two distinct Goethite and Hematite ores. Results from the initial benchmarking test campaign will inform the test program for a series of scouting trials to further explore the influence of the chemical, compositional and morphological properties of different iron ores and to provide critical data to inform the FEED study for a 30ktpa DRI ZESTY demonstration plant (Table 1).

Table 1 ZESTY campaign test matrix for goethite/hematite ores.

Intent		Goethite + Hematite Blends		
		Benchmarking Ore	Other Ores	
Identify different ore types suitable for Zesty technology	Finger printing in a finer range	PHASE 1	900, 950, 1000, 1050°C	TBD (2 temp)
	Particle size range		Dv0.8=100, 200, 300, 500 um	TBD (2 sizes)
Understanding the operation window for different ore	H ₂ ratio		H ₂ /O _{RED} = 1.2, 1.5, 2	TBD (2 ratios)
	Throughput		1, 1.6, 2 kg/min	TBD (2 rates)
Identify the possible additional steps/modifications	Pre-treatment	PHASE 2	Pre-calcination	N/A
	Pre-heating of H ₂		With optimised conditions	N/A
Collect quality data ZESTY FEED study	Select optimal condition and running till equilibrium		Optimised Conditions	Optimised Conditions
Generate sample for downstream testing				

Based on the outcomes of initial benchmarking test trials, critical parameters including process temperature, feed rate, and H₂/O_{red} ratio were ascertained to help streamline the optimisation process for attaining the highest possible metallisation extent. These parameters were utilised to develop the test plan for the G0503 ore as detailed in Table 2.

Table 2 Phase 1 test plan for G05 goethite and hematite blend ore.

No.	Raw Sample ID	Reactor Wall Setpoint T [°C]	Feed Rate (kg/min)	Feed quantity (kg)	(H ₂ / O _{RED})
1	G0503	950°C	1	20	1.5:1
2	G0503	1000°C	1	20	1.5:1
3	G0503	1000°C	1	20	2:1
4	G0503	1000°C	1	20	1.2:1
5	G0503	1000°C	1.6	20	1.5
6	G0503	1000°C	1.6	20	1.2
7	G0503	1000°C	1.6	40	1.5

3.2 Materials and Methodology

3.2.1 Materials

Goethite and Hematite Ore

Two goethite and hematite blend ores were employed, to assess the effect of Fe composition, gangue content and morphological differences on the milling and H₂ direct reduction behaviour. The ores are denoted as G01 and G05 respectively. Subsets of the ores, such as different milling specifications are denoted but a four-digit code e.g., G0109. These ores were selected as the main comparison for the pilot test work as despite both being goethite and hematite blends, both ores have different Fe composition, gangue composition and morphological differences that result in very different milling characteristics. The intent of this choice is to highlight any performance differences in the process between different ore bodies of similar minerals.

The mineral compositions of the G01 and G05 ores employed are provided in Table 3. XRF analyses were undertaken by ALS lab using a PANalytical (Model) sequential WDXRF spectrometer. The mineralogical composition of the iron ore is provided in

Table 4 (see 3.2.2 for XRD method). Particle size distribution (PSD) measurements were conducted using a Mastersizer 3000 (Malvern, Worcestershire UK) using ethanol as the dispersant. A particle refractive index of 2.56 and dispersant refractive index of 1.36 were used for all samples. Multi-elemental analyses were performed using ICP-MS analyses. Characterization detail can be found in section 3.2.2.

Table 3 Dominant mineral compositions of the goethite and hematite blend G01 ore used in the initial goethite and hematite blend ore benchmarking test and the G05 ore.

Mineral Elements and Oxides	Goethite / Hematite G01 Ore	Goethite / Hematite G05 Ore
Fe	55.85	60.90
SiO ₂	6.62	4.10
Al ₂ O ₃	3.28	2.49
C organic	0.17	0.08
LOI	8.24	5.36

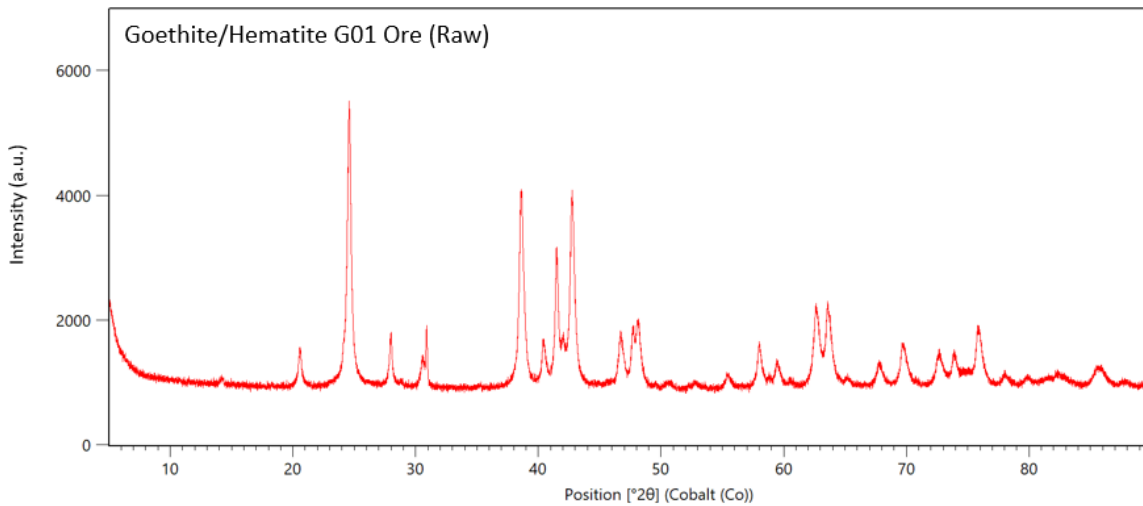


Figure 3 X-ray diffractogram of the goethite and hematite blend G01 assessed for initial benchmarking.

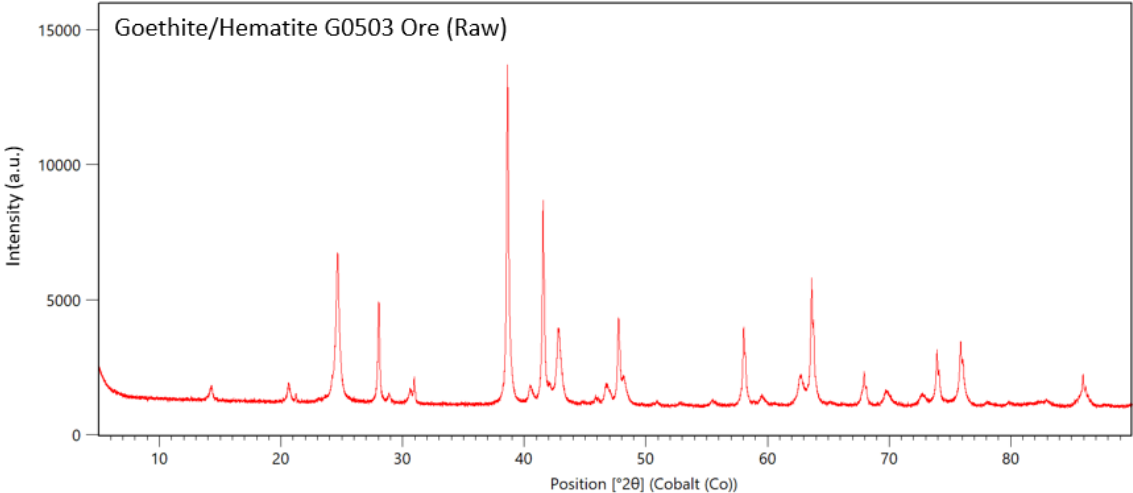


Figure 4 X-ray diffractogram of the goethite and hematite blend G05

Table 4 Mineralogical composition of goethite and hematite blend G01 and G05 ore by quantitative XRD.

Phase	G01 (wt%)	G05 (wt%)
Goethite	72.5	53.2
Hematite	23.9	43.1
Quartz	2.1	2.5
Other Gangue	balance	balance

The G01 ore, a blend of goethite and hematite, was milled to attain four PSD specifications: $d_{80} = 100 \mu\text{m}$, $200 \mu\text{m}$, $300 \mu\text{m}$, and $400 \mu\text{m}$. This milling was conducted by Micropowders in Victoria, Australia, using a roller mill. In contrast, based on initial benchmarking test results, the G05 ore sample aimed for a single d_{80} PSD specification of $200 \mu\text{m}$, also using a roller mill from Micropowders. The ore were processed in a batch mode; thus, the milled materials were homogenised to reduce variation between batches. After homogenization, the G0503 sample yielded a d_{80} value of $124 \mu\text{m}$, a variance attributed to the high fine concentrations and the material's mineralogy. PSD measurements of the G01 and G05 ores are presented in Figure 5 and Figure 6, respectively, and a summary of their PSD is detailed in Table 5.

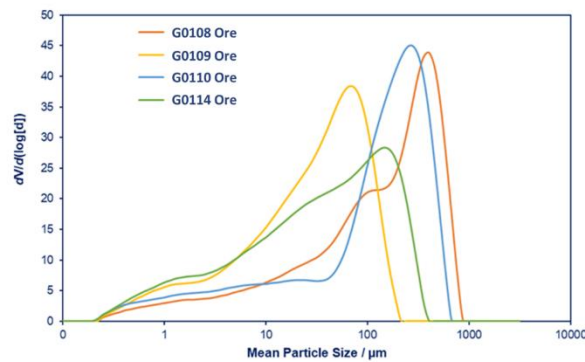


Figure 5 Particle size distributions (PSD) of the goethite and hematite blend G01 ore of different particle sizes using laser diffraction technique.

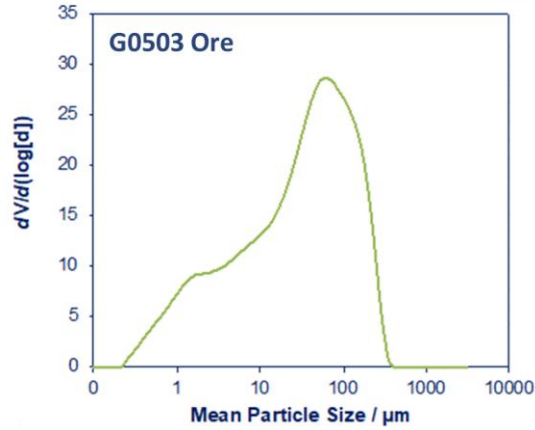


Figure 6 PSD of the goethite and hematite blend G0503 ore using laser diffraction technique.

Table 5 PSD summary of the goethite and hematite blend G01 ore of different particle sizes and the G0503 ore using laser diffraction technique.

Sample ID	Particle Size Distribution Summary [μm]				
	d_{10}	d_{50}	d_{80}	d_{90}	d_{99}
FeO-0108	7.6	189	474	604	857
FeO-0109	2.8	38.9	92.6	124	198
FeO-0110	4.3	177	361	461	662
FeO-0114	2.3	45.8	159	228	371
FeO-0503	2.07	41.4	124	185	323

Table 6 Specific surface area (SSA) and pore properties of the goethite and hematite blend G01 ores of different targeted particle size distributions assessed for initial benchmarking and the G0503 ore.

Sample ID	SSA [m^2/g]	N_2 Adsorption Measurements	
		Total pore volume [cm^3/g]	Mean pore diameter [\AA]
FeO-0108	9	0.03	19.14
FeO-0109	12	0.04	19.14
FeO-0110	10	0.04	19.13
FeO-0114	10	0.04	19.14
FeO-0503	9	0.05	19.14

3.2.2 Methodology

3.2.2.1 Particle size distribution (PSD)

Particle Size Distribution (PSD) was determined by utilising a Malvern PANalytical Mastersizer 3000 laser diffraction apparatus. Ethanol functioned as the dispersant medium. A refractive index of 2.58 was employed for the measurements. The specimen was incrementally introduced to the instrument until the observed obscuration range was within 10-20%. Prior to the measurement, a stabilisation period of one minute was allocated to ascertain thorough dispersion of the specimen in the dispersant.

3.2.2.2 Surface area analysis (SSA)

N₂-adsorption analysis was employed to determine the SSA, utilising a Quantachrome Autosorb iQ series instrument. An amount of 4 g of the sample was subjected to degassing in a vacuum before the analysis. The unprocessed hematite-goethite specimens were degassed at 80°C for 16 hours to avert decomposition. In contrast, the remaining samples were exposed to degassing at 200°C for 2.5 hours, with a temperature increment rate set at 20°C/min. The SSA was ascertained through the 11-point Brunauer-Emmett-Teller (BET) technique in the P/P₀ range <0.3 during adsorption stage. The pore volume was also evaluated using the Barrett-Joyner-Halenda (BJH) methodology for the desorption stage.

3.2.2.3 X-Ray diffraction (XRD)

X-Ray diffraction (XRD) was employed to investigate the structural characteristics of both the raw material and reduced DRI samples. The analysis was conducted using a PANalytical AERIS benchtop XRD instrument with a Cobalt target. Operational parameters included a maximum voltage of 40 kV and a current of 7.5 mA. The samples were subjected to scans within a 2θ range of 5° to 80°, taken in increments of 0.01°, with a counting duration of 29 s per step. Subsequent phase composition analysis was facilitated using the HighScore software.

3.2.2.4 Thermogravimetric analysis (TGA)

The thermogravimetric analysis (TGA) was employed to study the thermal decomposition behaviour of the sample using a Mettler Toledo TGA/DSC 3+ instrument. Approximately 50 mg of the sample was subjected to a temperature ramp from 25°C to 1000°C at a consistent heating rate of 50°C/min in an atmosphere of ultra-high purity nitrogen (N₂) with a purity level of 99.999%. The gas flow rate was maintained at 200 mL/min. A gas mixture of 10% H₂ and 90% N₂ was utilised to quantify how much reducible oxygen left in the samples.

3.2.2.5 Chemical assay (XRF & ICP-MS), Total Organic Carbon (TOC)

Samples weighing 5 g from the primary raw materials were subjected to external analysis to ascertain their elemental composition and quantify total organic carbon. The evaluations were performed at

Australian Laboratory Services Pty Ltd, a laboratory accredited by NATA in accordance with ISO/IEC 17025 standards. Elemental quantification was executed using X-ray Fluorescence (XRF) via the Fusion method. Inductively Coupled Plasma Mass Spectrometry (ICP-MS) was utilised to assess the presence of 48 distinct elements. Prior to these analyses, the samples underwent four acid digestions. Total Organic Carbon (TOC) was determined through preliminary dilute acid digestion, succeeded by combustion.

3.2.2.6 ZESTY Reduced Iron Ore Reduction Degree Calculation

The TGA H₂ reduction degree measurement is employed to estimate the reduction degree of ZESTY reduced iron ore products. Figure 7 demonstrated that samples were heated to 1000°C in an N₂ atmosphere.

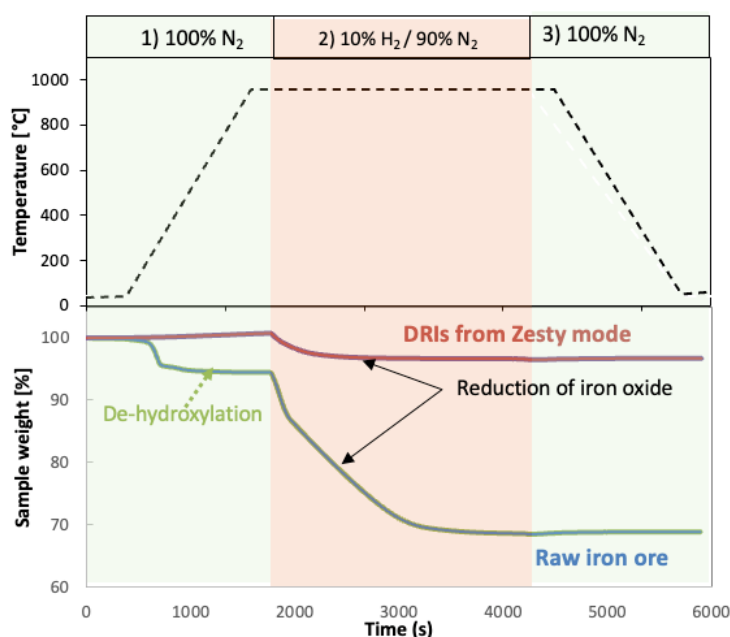


Figure 7 TGA-H₂ reduction extent measurement profile

The purge gas was then changed to a 10% H₂ and 90% N₂ mix at 200L/min. During this phase, weight loss due to the reaction between reducible oxygen (O_{RED}) and hydrogen was measured for 40 minutes at a consistent 1000°C. Post-reduction, the environment was switched back to N₂ and samples were cooled to 40°C before removal from the furnace. The Reduction Degree was calculated using equation 1 by comparing reducible oxygen concentration per unit mass between the initial iron ore feed sample (O_{RED-FEED}) and the Zesty reduced product sample (O_{RED-PRODUCT}).

$$\text{Reduction Degree (\%)} = 100 \times \frac{O_{RED-PRODUCT}}{O_{RED-FEED}} \quad (\text{Eq. 1})$$

The concentration of reducible oxygen (mol/g_{O_{RE-RED}}) was determined based on equation 2. This estimation involves the division of the weight loss observed during the TGA reduction phase by the atomic mass of oxygen. The resulting value is then normalised to the final weight of the fully reduced sample, represented as the weight of the sample (W_{RED}) at the termination of the reduction phase.

$$\text{Reducible Oxygen } (O_{RED}) \text{ (mol/g}_{ORE-RED}\text{)} = \frac{\Delta W_{RED} / A_{rO}}{W_{RED}} \quad (\text{Eq. 2})$$

Where:

1. ΔW_{RED} represents the weight loss measured during the TGA reduction period.
2. A_{rO} signifies the atomic mass of oxygen.
3. W_{RED} denotes the weight of the sample at the end of the reduction period.

3.2.3 Material Recovery Calculation

Material recovery/collection efficiency equates the ratio of the actual amount of material obtained at the product collection drum at the base of the ZESTY pilot plant (bulk sample) to the theoretical quantity expected for the given reduction conversion degree.

Material collection efficiency was calculated using the following formula:

$$\text{Collection efficiency (\%)} = 100 \times \frac{W_{bulk}}{W_{theory}} \quad (\text{Eq. 3})$$

$$W_{theory} = w_0 * (1 - LOI_{cal} - LOI_{red} \times \eta_{red}) \quad (\text{Eq. 4})$$

Where:

1. w_{bulk} is the bulk sample weight.
2. w_0 is the feed amount into the reactor.
3. LOI_{cal} is the total weight loss ratio due to calcination.
4. LOI_{red} is the total weight loss ratio due to the reduction of raw ore.
5. η_{red} is the reduction degree obtained by (Eq. 2)

3.3 Campaign Results for Goethite and Hematite Blend G01 and G05 Ores

3.3.1 The Effect of Temperature on Reduction Degree and Collection Efficiency

The initial benchmarking testing was undertaken at a feed rate of 1kg/min and H₂ flow rates selected to provide a H₂ stoichiometric ratio of 2:1 at a temperature range of 900 to 1050 °C with the goethite/hematite G0114 ore milled to a PSD target specification of d₉₀ = 230 μm. An increase in temperature between the 900 to 1050°C temperature range facilitated an increase in the reduction for G0114 ore. On the contrary, a similar trend of progressive increasing trend was not observed in the metallisation degree measurement. From the metallisation degree data presented in Figure 8, increasing the temperature from 900-1000°C did not materially impact the metallisation where an increase in metallisation was achieved when the temperature was further increased to 1050°C. Furthermore, as depicted in Figure 8, the collection efficiency was only enhanced up to 1000 °C before it started to drop off at 1050 °C.

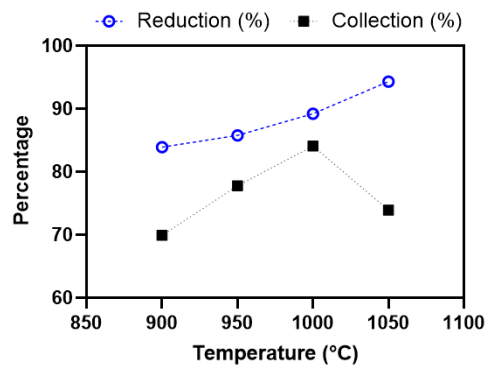


Figure 8 Reduction degree and material collection efficiency tested with various temperatures for the G01 ores FeO-0114 at an H₂ ratio of 2:1 and a 1 kg/min feed rate.

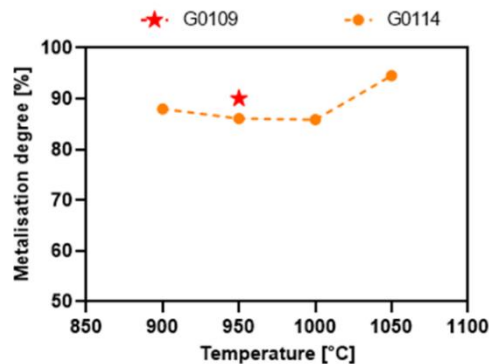


Figure 9 Metallisation degree tested with various temperatures for the G01 ores FeO-0114 and G0109, at an H₂ ratio of 2:1 and a 1 kg/min feed rate.

Upon reaching 1050 °C, product aggregation and fusion instances were observed. However, PSD measurements yield no evident aggregation, with the exclusion of big clumps larger than millimetre scale (shown in Figure 12). The decline in collection efficiency at 1050 °C is theorised to be a consequence of material adherence to the reactor wall, with the clumps potentially emanating from fused materials detached from the reactor wall. The increase of collection efficiency from 900 to 1000°C is still under investigation, potential reasons include such as densification of material and less breakage of particles at high temperatures.

Therefore, based on the outcomes from the benchmarking test using the G01 ore, processing temperatures of 950 °C and 1000 °C were selected for the G0503 ore. These choices showed congruence (i.e., higher than 80% reduction degree and increasing collection efficiency at higher temperature) with the outcomes observed for the G01 ore, shown in Figure 10. As the temperature increased, there was a noted enhancement in collection efficiency. However, both conditions witnessed a diminution in fines, as depicted in Figure 11.

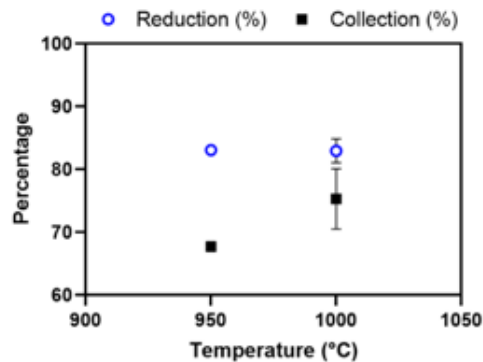


Figure 10 Reduction and material recovery tested with G0503 at 950°C, H₂/Ored ratio of 2:1, feed rate of 1 kg/min.

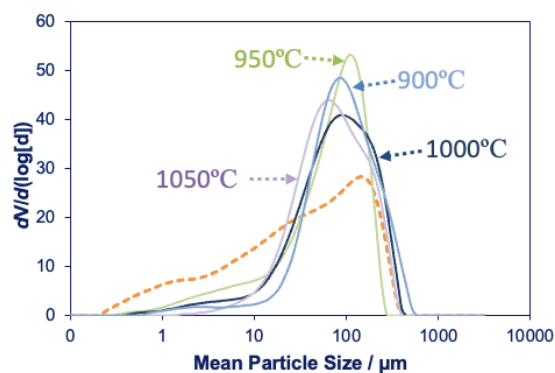


Figure 11 PSD results of samples from G0114 reduced at various temperatures with an H₂ ratio of 2:1 and a 1 kg/min feed rate.



Figure 12 Clumps were formed in the processed G0114 DRI at 1050°C.

3.3.1.1 2023 ZESTY Campaign Results to 2022 Proof-of-Concept Campaign

Early results from the initial benchmarking campaign for the G01 goethite and hematite blended ore milled to a PSD specification of (d90 = 124 μm and 228 μm) (Table 7) show a high level of consistency between the reduction degree measurements from the 2022 campaign, (presented at the ESTAD/METEC conference (1)) and the results of the latest goethite/hematite blend G01 ore benchmarking campaign (Figure 13 PSD measurements of the ores employed in the 2023 ZESTY campaign compared to the goethite/hematite HG57 ore used during the 2022 proof-of-concept campaign.) A consistent improvement in reduction degree is observed with increasing temperature between 900 to 1050 °C exceeding 90 mol% for both particle size ranges.

Table 7 Specifications of the milled G01 goethite and hematite blended ore milled to a target particle size specification of (d80 = 100 μm and 200 μm)

	Ore type	Fe (wt%)	D90 (mm)	SSA (m ² /g)	Pore Volume (cm ³ /g)
a)	Siderite (FC43)	42.7	85	25	0.04
b)	Goethite/Hematite (HG57)	56.4	130	15	0.03
c)	Goethite/Hematite (HG59)	59	130	14	0.04
d)	Magnetite (Ma68)	67.7	40	0.8	0.003
e)	Goethite / Hematite (G0109)	56	124	11.7	0.04
f)	Goethite / Hematite (G0114)	56	228	10.2	0.04
g)	Goethite / Hematite (G0503)	60.9	185	9	0.05

Note: Goethite/Hematite (G01 and HG57) ores were sourced from the same supplier and product line as G01 ore. a) to d) were tested in the 2022 ZESTY campaign, Goethite/Hematite (G0109, G0104, and G0503) ores were employed for the 2023 ZESTY campaign (highlighted in blue).

The materials recovery from previous campaign was consistently low due to the entrainment of fine particles in the off-gas. Figure 1 addresses this, a cyclone and baghouse were installed at the exhaust outlet to separate and return the elutriated particles to the process for improved materials recovery. As evident from Figure 13, the material recovery results for the HG57 ore from earlier campaign and recent results with the G0109 ore which share similar PSD specifications and are derived from the same supplier and product line provide an early indication of the positive effect of the cyclone and baghouse modification whereby the materials recovery efficiency increase from 38 % to 51%. Moreover, by increasing the particle sizes, product collection efficiency can be marginally improved further (e.g., the collection efficiency with D90 of 228 μm achieved 78% under the identical test condition). Although this is not completely resolved in this test campaign, it is believed that collection efficiency can be further improved by fine-tuning the gas flow and optimise the crushing & milling process.

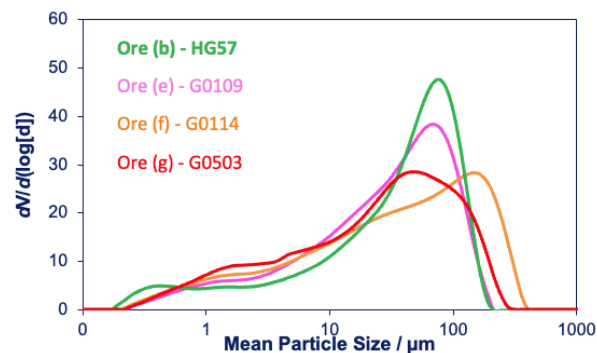


Figure 13 PSD measurements of the ores employed in the 2023 ZESTY campaign compared to the goethite/hematite HG57 ore used during the 2022 proof-of-concept campaign.

The alignment between the 2022 and 2023 results (as depicted in **Error! Reference source not found.b)** indicates a strong degree of reproducibility in the testing procedures across the two campaigns.

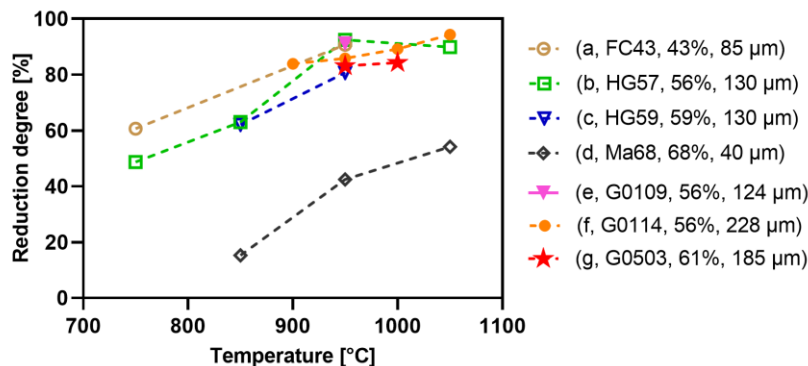


Figure 14 Metallisation degree as a function of wall temperature setpoint. (Ore type = various; T_{wall} = variable; Feed rate = 1 kg/min; H_2 stoichiometric ratio = 2 for ores a-f and 1.5:1 for g)

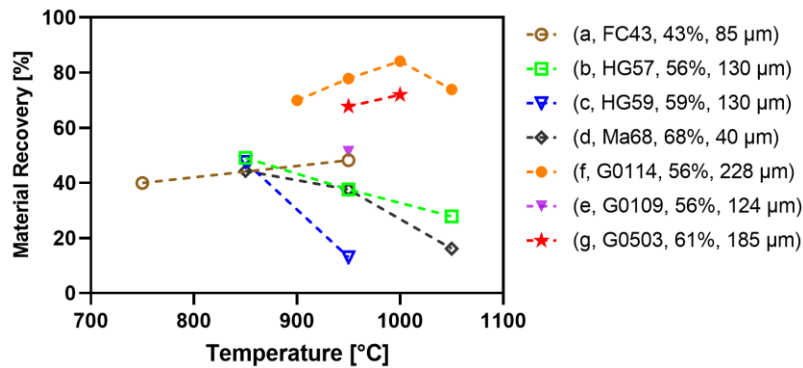


Figure 15 Reduction degree of reduced products as a function of wall temperature setpoint. (Ore type = various; T_{wall} = variable; Feed rate = 1 kg/min; H₂ stoichiometric ratio = 2 for ores a-f and 1.5:1 for g).

3.3.1.2 Effect of Ore PSD (Milling Specification) on the Reduction Degree and Materials Recovery

A strong inverse correlation between reduction degree and material recovery can be observed from the initial benchmarking G01 ore trial results from a $d_{80} = 95 \mu\text{m}$ to a $d_{80} = 475 \mu\text{m}$ shown in Figure 16. The product reduction degree reduces as the particle size of the feed material increases, whilst material recovery exhibited an inverse trend. It worth noting that the metallisation degree and reduction degree are very consistent, further confirming the trade-off between the material recovery and conversion with this set of test condition.

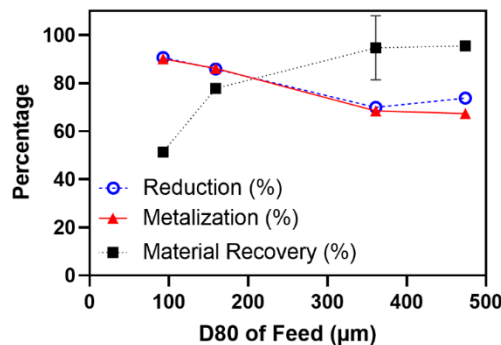


Figure 16 Reduction, metallisation, and material recovery tested with various particle sizes at 950°C, H₂/Ored ratio of 2:1, feed rate of 1 kg/min.

The sub-optimal material recovery rate for finer materials is attributable to the high gas velocities' loss of ultrafine fractions below 100 μm. The bulk samples collected at the bottom of the reactor (b and c) showed substantially lower fines in its PSD, evidenced in Figure 17. However, no indication of

agglomeration or decrepitation was discerned. A possible explanation for the observed phenomenon is the transportation of fines into the dedusting system by the upward-moving process gas. Despite the re-entry of these fines into the reactor from the top, their lightweight nature, characteristic of fine particles, predisposes them to be recirculated back into the dedusting system, thereby potentially resulting in a perpetual loop during each trial. Further studies are required to gain better understanding on the behaviour of the fine materials in the pilot reactor system.

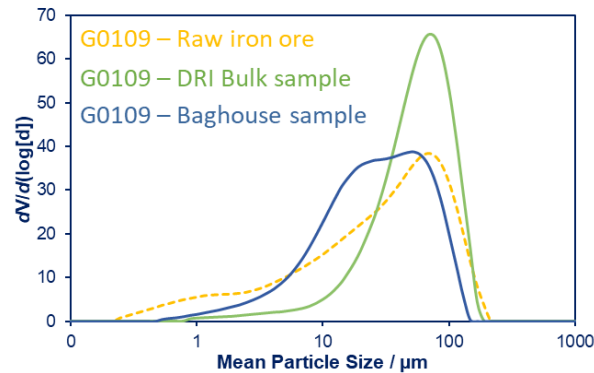


Figure 17 PSD comparison of raw, bulk, baghouse, and cyclone samples from G0109 reduced at 1000°C, H₂/Ored ratio of 2:1 and feed rate of 1 kg/min.

An assessment of the reduction degree of powder samples, collected from the off-ga (via cyclone and baghouse) revealed the reduction degree was significantly lower than that of the equivalent bulk product sample (26 mol% and 37 mol% vs 89 mol%, respectively, shown in Table 8). This disparity indicates an early elutriation of particles within the process and a shortened residence time of the elutriated powder. Additionally, a significantly higher surface area was measured, which suggests a lesser extent of sintering. This metric further verifies the hypothesis of early elutriation during the process.

Table 8 PSD and reduction degree of raw, bulk, baghouse, and cyclone samples from G0109 reduced at 1000°C, H₂/Ored ratio of 2:1 and feed rate of 1 kg/min

	Reduction [%]	SSA [m ² /g]	D10 [μm]	D50 [μm]	D80 [μm]	D90 [μm]
Raw Feed	-	10.2	2.28	45.8	159	228
Baghouse	36.8	26.9	7.13	34.7	80.2	108
Cyclone	25.8	N/A	13.7	48.7	87.7	113
Bulk	89.2	1.5	19.6	93.5	200	267

Examination of the PSD profiles of off-gas samples revealed a significantly elevated fraction of fines compared to feed, with the maximum particle size parking around 50 μm. This demonstrates a

pronounced propensity for elutriation of fine particles below the threshold of 50 μm , thereby contributing to the loss of materials in fine fractions.

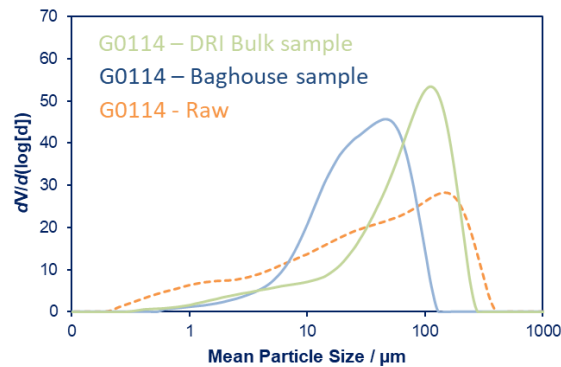


Figure 18 PSD comparison of the raw, bulk sample and off-gas sample from the G0114 ore.

The incorporation of upgrades, namely the cyclone and baghouse, engendered an amelioration in material collection by facilitating the re-injection of captured fines. Despite implementing upgrades on the pilot reactor to capture and recirculate the fine particles, a notable degree of elutriation was observed due to high gas flow which resulted in a loss of fines portion in the final bulk sample. Hence, a comprehensive understanding of these dynamics is instrumental for devising strategies to optimise material recovery and reduction degree further, aligning with the overarching objectives of the ZESTY pilot plant testing campaign.

3.3.1.3 The Effect of Feed Throughput and H₂ Stoichiometry Ratio and Flow on Reduction Degree

During the initial benchmarking trials using the G0114 ore (D₈₀=159 μm), the current investigation evaluates the implications of throughput and H₂ stoichiometry on two dependent variables, the reduction degree and collection efficiency in the BATMn reactor system. The throughput parameter varies within the 1.0 to 2.0 kg/min range. Notably, as depicted in Figure 19, the increasing throughput while maintaining a 2:1 H₂ stoichiometry is analysed. It is found that this combination has a marginal effect on the reduction degree for material collected at the base of the reactor but results in a decrease in material recovery. This is presumably due to the increased flow rate of the gases within the system. The PSD measurements of the reduced products reveal a marginally narrower particle distribution due to the removal of fine particles, as illustrated in Figure 20. Figure 20 PSD results from various H₂ ratio (labelled in figure) for the ore G0114, at 1000C and feed rate of 1.6 kg/min. When the feed rate rises from 1.0 to 2.0 kg/min, fractions measuring below 45 μm reduce from 11% to 5%. Similar trend was also observed between metallisation degree and material recovery depicted in Figure 19b.

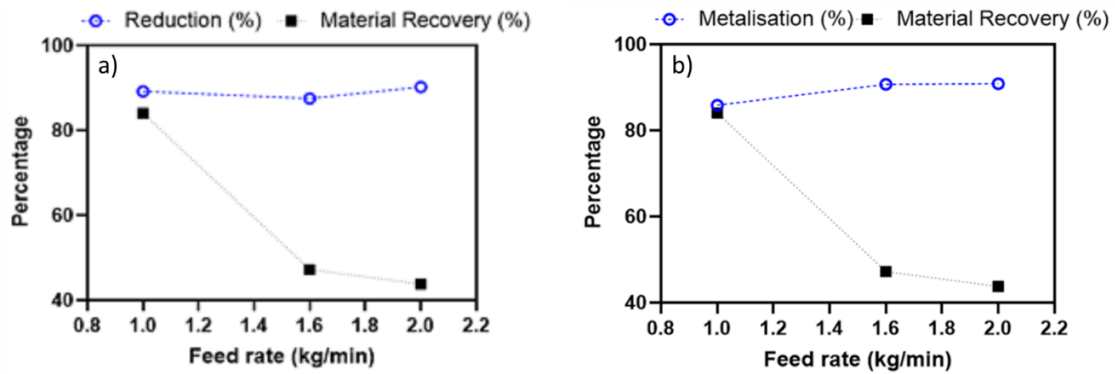


Figure 19 a) Reduction and material recovery b) metalisation and material recovery tested with various H2 ratio for the ore G0114, at 1000C and feed rate of 1.6 kg/min.

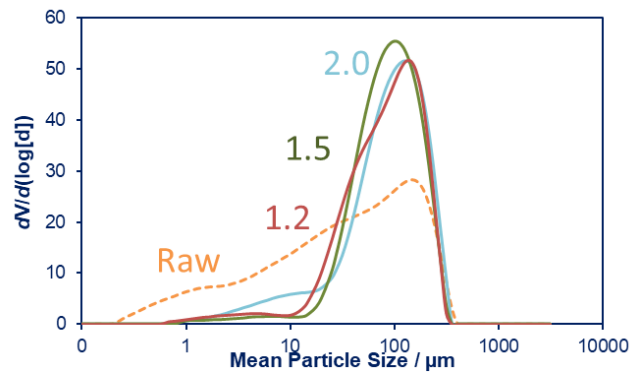


Figure 20 PSD results from various H2 ratio (labelled in figure) for the ore G0114, at 1000C and feed rate of 1.6 kg/min.

To maintain a consistent H₂ stoichiometry of 2:1 in response to higher throughput, the H₂ inflow is adjusted in proportion to the feed rate. This adjustment results in the elongation of pre-heating zones for both powder and H₂ within the reactor. Consequently, the length of the zone that maintains full temperature is reduced. Yet, despite this reduction, the higher H₂ flow rate may extend the residence time within each zone. This hypothesis of extension in residence time agree with a decline in SSA as feed rate increases which can be seen in Figure 21. This is towards the lower end of the instrument sensitivity so further work will be undertaken to understand this correlation and the trade-offs between gas flows, residence times and metallisation. Furthermore, as can be seen from Figure 22, the collection efficiency for the G0114 ore declined significantly, dropping to 44% when the throughput is adjusted to 2.0 kg/min, potentially due to increased powder elutriation driven by increased superficial gas flow.

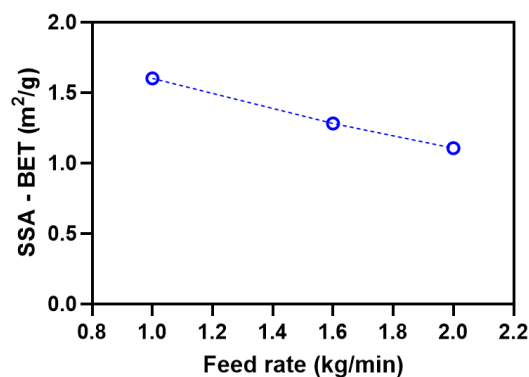


Figure 21 Specific Surface area of DRI samples generated from various feed rates for the ore G0114, at 1000 °C, H₂ ratio of 2:1.

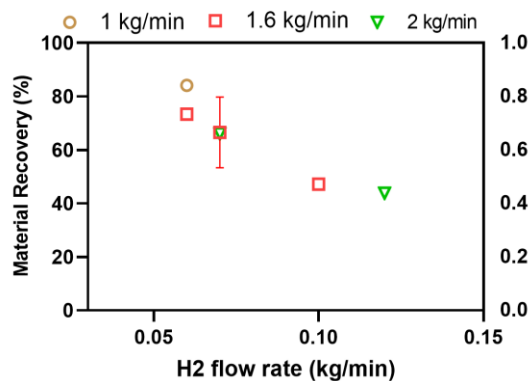


Figure 22 Material recovery performance under various feed rates under different H₂ flow rates for the ore G0114, at 1000°C, H₂ ratio of 2:1.

A separate examination is conducted to assess the effects of altering the H₂ stoichiometry on the G0114 ore, presented in Figure 23 and Figure 24a. Specifically, the reduction from stoichiometry of 2 to 1.5 positively impacts material recovery, without any observable impact on the reduction degree. In contrast, a further reduction to a stoichiometry of 1.2 results in a diminished reduction degree, an outcome that may be explained through multiple influential factors, including a decrease in the kinetic driving force, thermodynamic limitations, and reduced residence time within the reactor. Similar trends

were observed in the metallisation degree for the stoichiometry of 1.5 and 1.2 when compared to the reduction degree performance at the same H_2/O_{red} ratio. In Figure 24, it is suggested that the degree of metallisation could be lower than expected at a feed rate of 1kg/min at a stoichiometry of 2. The data trend also indicates the degree of metallisation, showing values potentially higher than those observed at 1kg/min. However, further testing is still required to confirm the repeatability and the significant role of feed rate on material recovery, which make it difficult to draw definitive conclusion regarding metallisation performance on the current data set.

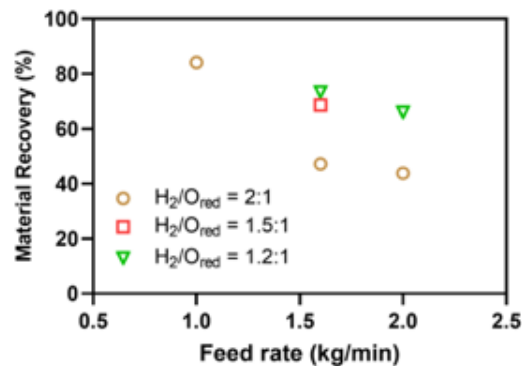


Figure 23 Material recovery tested with various feed rates for the ore G0114, at H_2/O_{red} ratio at 1000°C.

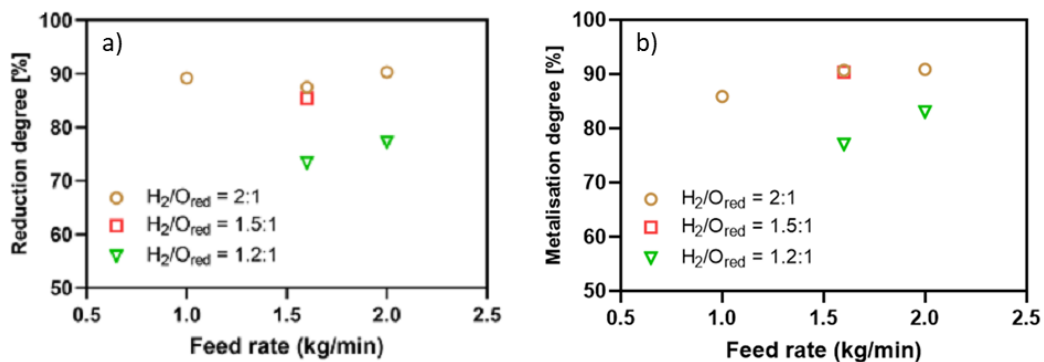


Figure 24 . a) Material reduction degree b) metallisation degree tested with various feed rates for the ore G0114, at H_2/O_{red} ratio at 1000°C.

As for the G0503 ore, Figure 25 shows that an increase in the H_2/O_{RED} ratio typically led to an increased reduction degree, consistent with the findings from the benchmarking G/H ore test trials. Nonetheless, the material reduction degree observed at 1.0 kg/min and an H_2 ratio of 1.2 deviated from the prevailing trend. Without subsequent investigative trial tests, this observation will temporarily remain without a comprehensive explanation.

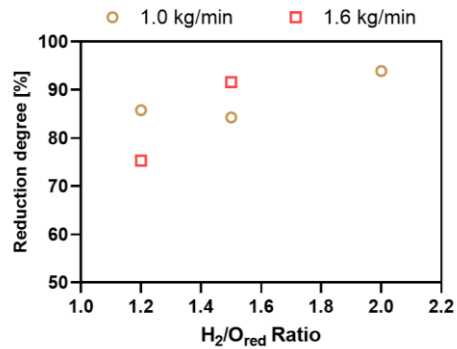


Figure 25 Reduction degree tested with various H₂/O_{red} ratios at 1kg/min feed rates and 1.6kg/min for the ore G0114, at 1000°C.

At a feed rate of 1.6 kg/min in Figure 26, the observed reduction degree at an H₂ ratio of 1.2 registered approximately 75%, considerably lower than the 91.6% documented at an H₂ ratio of 1.5. Concurrently, the material collection declined slightly from 61% to 58%, as depicted in Figure 26. In contrast, with a 1.0 kg/min feed rate, the material collection efficiency remained relatively constant across varying H₂/O_{RED} ratios.

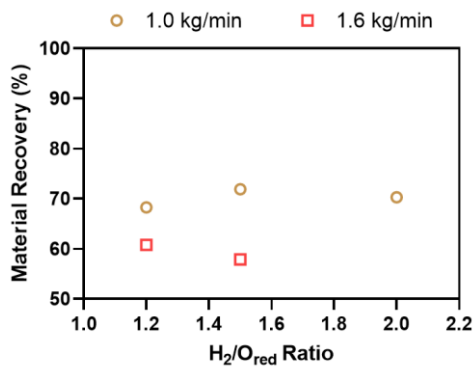


Figure 26 Material recovery tested with various H₂/O_{red} ratios at 1kg/min feed rates and 1.6kg/min for the ore G0114, at 1000°C.

A noticeable trend shown in Figure 27 revealed the decline in material recovery corresponding to an increase in H₂ flow rate, aligning with observations from the initial G01 ore benchmarking trials.

Notably, all DRI products exhibited a nearly uniform particle size distribution across the examined parameter range: temperatures of 950 and 1000 °C, H₂ ratios spanning 1.2 to 2.0, and feed rates ranging from 1.0 to 1.6 kg/min.

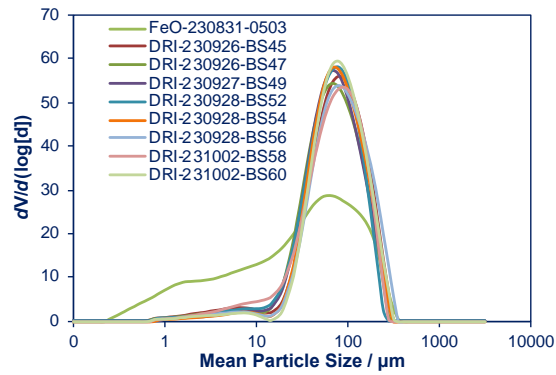


Figure 27 PSD comparisons between the unprocessed 0503 ore and the DRI samples produced from the G0503 ore under various trial conditions.

4 BRIQUETTING AND SMELTING TRIALS UPDATE

As part of this FEED (front end engineering design) study, two options are being explored for the downstream processing of hydrogen direct reduced iron (H-DRI) fines resulting from Calix' ZESTY (zero emissions steel technology) process. The first option is hot briquetting resulting in hot briquetted iron (HBI) and the other downstream processing option involves putting the hot DRI through a smelting furnace.

Calix Ltd have identified Köppern, Germany as a potential vendor with appropriate knowledge and experience with the post processing of DRI to produce hot briquetted iron (HBI).

Furthermore, Swinburn University will be a research partner for the duration of the FEED study and will be assisting Calix with compaction and melting experiments using DRI produced from the ZESTY testing campaign at Bacchus Marsh.

4.1 Hot Briquetted Iron (HBI)

The production of fine DRI involves a reduction reaction whereby oxygen is removed from iron ore. This results in the formation of sponge iron (DRI) which is highly porous. Given the large specific surface area of DRI, it is highly reactive with oxygen and/or water. The reaction with oxygen is highly exothermic and can result in overheating, meltdown of DRI stockpiles, silos, ship holds. The reaction with water produces hydrogen which generates explosive mixtures with air.

Given the high risks associated with storing and transporting DRI, methods of passivation have been developed. One of the most reliable processes for passivation of DRI is hot briquetting; immediately after reduction, the DRI is densified at high temperatures and pressures. The hot briquetting process results in DRI with reduced porosity, increased apparent density and improved thermal conductivity – all of which reduce reactivity. Briquetted DRI is considered safe for storage and transportation.

Hot briquetted Iron has the following potential advantages:

- Minimal loss of metallisation
- No issues with open air storage
- Minimum risk of overheating during storage and transportation
- Inertization of ship holds are not required.
- High apparent and bulk densities
- Low moisture saturation
- Efficient preheating for electric arc furnace (EAF) is possible.

4.1.1 Hot Briquetted Iron (HBI) test work plan

Through ongoing discussions with Köppern, it was decided that samples of DRI from the current ZESTY campaign will be sent to a Köppern material testing facility in Germany whereby it would undergo numerous tests to assess the suitability of Calix' DRI for hot briquetting.

Köppern have recommended piston press testing for Calix' DRI samples. The piston press testing will be performed at various temperatures and pressure. The following properties will be identified as part of the testing program:

Feed Material:

- Bulk density
- Apparent density
- Absolute density
- Grain size distribution
- Pore size distribution

Briquette Quality:

- Apparent density
- Abrasion resistance
- Briquette thickness
- Compression strength

Pressing Process:

- Compression work
- Densifying ratio
- Densifying efficiency
- Briquette height under pressure
- Compression ratio

4.1.2 Direct Reduced Iron (DRI) – sample transport and testing update

At this stage of the project, sufficient sample quantities as required by Köppern for the HBI test work have been gathered from the current ZESTY testing campaign at Calix' Bacchus Marsh facility. The DRI samples are classified as dangerous goods, and this involves special packaging and shipping requirements. Calix have engaged Rhenus Logistics who specialise in transporting dangerous goods to assist with the transportation of the DRI samples.

The DRI samples will be transported from Calix's site at Bacchus Marsh, Victoria to Köppern testing facility in Freiberg, Germany. The DRI samples have been dispatched in October 2023 and the agreed upon Piston Press testing of the DRI samples is expected to take place in November 2023.

5 COMPETITIVE TECHNOLOGIES ASSESSMENT

This section has been prepared with the engagement of Geoffrey Brooks and Shabnam Sabah from Swinburn University of Technology to leverage their expertise and retain objectivity when comparing the ZESTY technology with other technologies on the market.

5.1 Introduction

The Blast Furnace (BF) process is the dominant ironmaking technology today. There are other alternate technologies available such as coke/coal-based technologies (Technored, Hismelt, Hlsarna, COREX, FINEX), gas-based options with integration of hydrogen (MIDREX shaft furnace, HYL/Energiron, HYBRIT, Circored, FINMET) and plasma and electrolysis-based ironmaking. At present, Iron and steelmaking Industry worldwide is going through the transition of decarbonisation to meet its goal of reaching net zero by 2050. The BF is energy intensive (15.28 GJ/tls) and there are concerns over the large CO₂ emission associated with coke-based BF operation. Adoption of other ironmaking technologies such as direct reduction and smelting reduction process are growing as there is a push to reduce emissions and lower energy consumptions. In this context, there is a general drive to adopt hydrogen in the reduction process. Hydrogen is considered as the most promising clean energy due to its high calorific value, good thermal conductivity, and high reaction rate (2). Though full application of H₂ in either blast furnace or other alternate ironmaking processes is an economically and technologically challenging, it has the most environmentally promising goal for decarbonisation. As an alternative reductant, H₂ has a faster reduction rate than CO, and the product (water) makes it the best fuel to reduce CO₂ emissions (3).

Flash smelting has been used in the field of copper and nickel production since its commercialisation in 1950s (4). Sohn and his co-workers brought this concept into ironmaking in early 2000 (5) where iron is produced from iron ore concentrates using flash reduction reaction. Currently, there is a novel H₂ direct reduction flash iron-making technology called Zero Emissions Steel Technology (ZESTY) under development where iron ore fines (typically < 500µm) are turned into DRI without pelletisation or agglomeration. Due to the small particle size, the rate of metallisation is quicker and have shorter residence time (in the order of 60s) (1) In the following sections, ZESTY and its competitive technologies have been briefly described and compared based on the characteristics of the process, techno-economic comparison, technological readiness level and emission reduction potential.

5.2 Zero Emissions Steel Technology (ZESTY)

The ZESTY process is indirectly heated. Since it can handle intermittent operation, renewable energy sources can be used for heating. It is based on the proprietary Calix Flash Calcination (CFC) technology. The iron ore fines are heated and reduced to DRI as it travels through the tubes of the reactors (as shown in Figure 28). Then it can be briquetted to sell as a Hot Briquetted Iron (HBI) to steelmakers or melted in the melting unit to remove gangue from the iron (1)

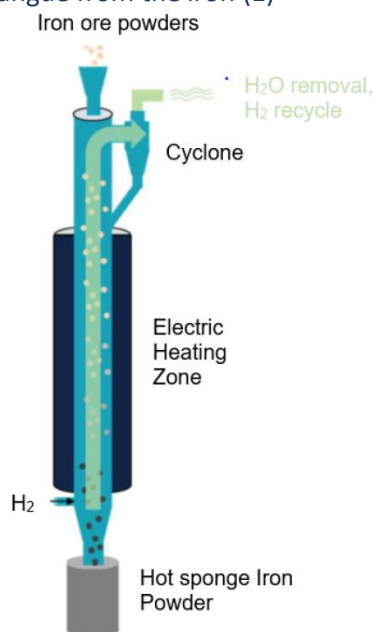


Figure 28 Schematic of the ZESTY reactor (1)

In this process, H₂ is used as the reductant, not as a fuel. Given the present cost of H₂ is high, the process is thus more economic and efficient. ZESTY aims to apply stoichiometric amount of H₂ (i.e., 54 kg/t) to reduce hematite ore and have employed recirculation loop for the unused H₂ back into the reactor. There is a provision for a cyclone and dedusting system by which iron ore fines that are entrained in the exhaust gases can be fed back into the process (1).

5.3 Description of the Competitive Technologies

There are several technologies that are competitive with ZESTY based on the feed materials, reducing gas, techno-economics, and emission reduction potential. The competitive technologies are described in the section below.

5.3.1 Flash Ironmaking Technology (FIT)

A novel flash ironmaking technology was developed at the University of Utah, called flash ironmaking technology (FIT). This technology does not require pelletizing/sintering steps which is needed in Midrex and Energiron ironmaking technologies. It is different from fluidised bed technology where iron ore “fines” are used with particle size of +0.1 mm to -10 mm. The FIT use iron ore concentrates with mean diameter less than 100 μm in size. Typical iron ore concentrate size used in this process is between 25 to 32 μm [(6) (7) (5)]. This process uses natural gas, hydrogen, or mixture of both and does not need coke, pellets, or sinters. It significantly decreases consumption of energy by 30 to 60% and reduced emission of CO_2 by 60 to 96% compared to BF, depending on the usage of hydrogen (8).

5.3.1.1 Description and development of the process

In this process, the fuel gas is burnt partially with O_2 which produces a reducing gas (as shown in Figure 4) at a temperature of 1200 to 1600 $^\circ\text{C}$. Iron ore concentrate is fed into the flash shaft from the top. Reduction of the ore takes place as they move downward. This process can create molten-iron bath for possible direct steelmaking or produce solid iron particles to be charged into the steelmaking process.

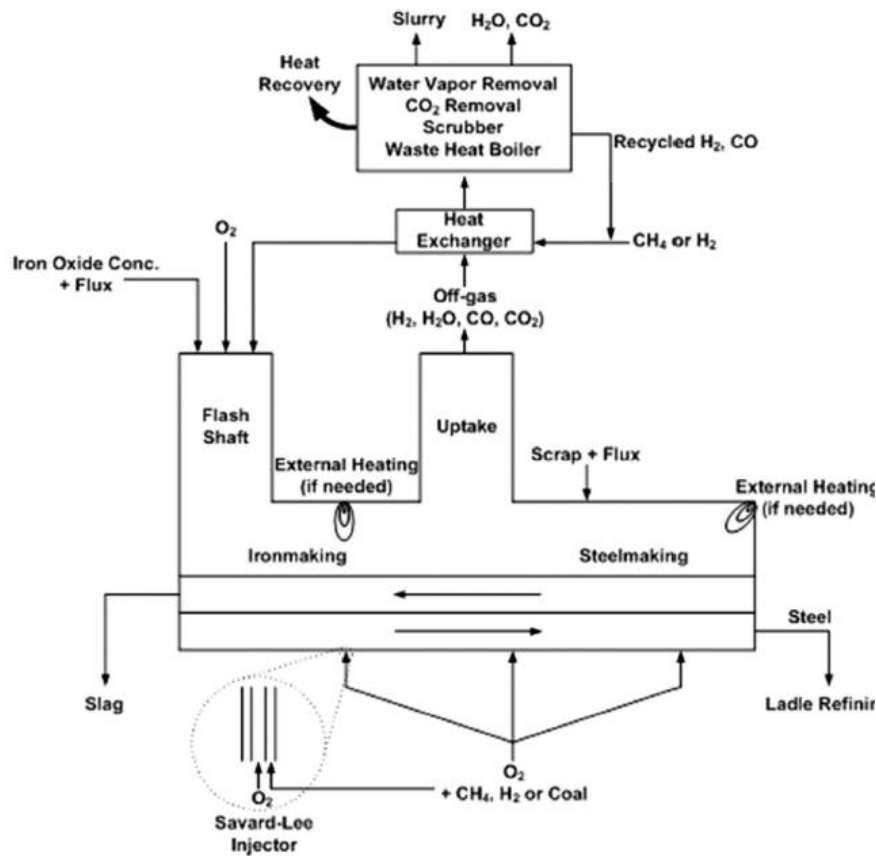


Figure 29 A schematic diagram of flash ironmaking and a possible direct steelmaking process (8) (9)

The process has been going through various stages of development. It has been simulated in a laboratory flash reactor and results were compared by CFD simulation. A pilot plant flash reactor (PFR) was built at the university of Utah based on the findings of laboratory flash reactor. A medium sized reactor with a capacity of 100,000 t/y of iron was built by computational fluid dynamics (CFD) modelling to collect information on the temperature and species distribution, gas, and particle flow patterns which are essential for any reactor design. Finally, Industrial Flash Ironmaking Reactors producing 0.3 and 1.0 million t/y of iron were designed by CFD modelling.

5.3.1.2 Laboratory Flash Reactor and CFD simulation

After the kinetic feasibility tests, Sohn et al. carried out reduction tests in a laboratory flash reactor [(5), (7), (8)] (as shown in Figure 30). Though there would be differences between an industrial flash reactor and a laboratory flash reactor in terms of sources of heat and low amount (20% to 100%) of excess reducing gases compared to the industrial process, the laboratory flash reactor had many features that represents an industrial flash reactor. Figure 5 shows the laboratory flash reactor at the University of Utah. It is consisted of an electrical furnace housing a stainless-steel tube, a gas delivery system, a powder feeding system, a power control system, an off-gas scrubbing system, and an off-gas burner. The electrical furnace housed a 316 stainless-steel tube with 19.5 cm ID and 213 cm length. The particles

were fed into the top of this reactor with two different feeding modes such as (a) feeding through the center of the fuel/oxygen burner; (b) feeding through two ports on opposite sides of the burner. Hydrogen or methane were used in the experiments with different modes of gas and particle feeding and then the results were analysed using computational fluid dynamics (CFD) simulations. Few findings of this investigation are as follows (5), (7), (8)]

Iron can be produced using iron concentrates by flash reduction using hydrogen, natural gas, or a mixture of both gasses.

The configuration of fuel gas and oxygen feeding as well as concentrate feeding mode is quite important for temperature distribution. The best position for concentrate feeding is near but outside the flame.

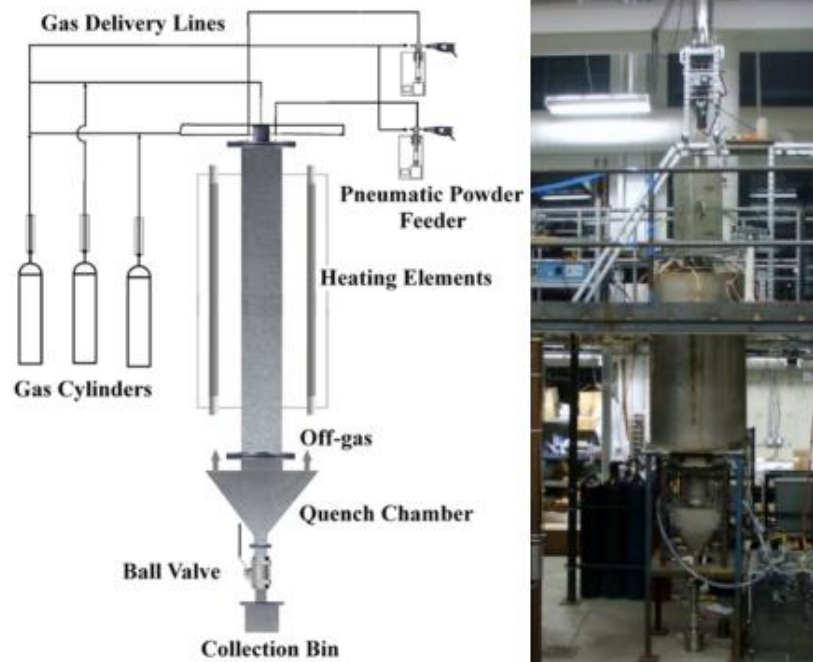


Figure 30 Laboratory flash reactor (7) (8)

5.3.2 Pilot Plant Flash Reactor

Pilot flash reactor (PFR) (as shown in Figure 31) was built at the University of Utah with iron ore concentrate feeding rate of 1–7 kg/h and operating temperature of 1200 to 1600°C (8). In this reactor, heat and reductant are produced by partial oxidation of natural gas or hydrogen with oxygen. The PFR had 3 types of burners such as a preheat burner, a main burner, and a plasma burner. Magnetite ore concentrate was fed into the reactor using a pneumatic powder feeder. Nitrogen gas was used as the carrier gas and was put into the reactor with a flow rate of 11 standard litres per minute (SLPM). The particles were fed through feeding inlets on the sides of the main burner. A leak test was carried out by capping the off-gas pipes and keeping the system at 2.0 atm pressure for 45 min. The system was preheated to the target temperature with a heating rate of 90–95 °C/h (8).



Figure 31 Pilot plant flash reactor (8)

5.3.3 Medium Sized Flash Ironmaking Reactors

Medium sized reactors were designed using CFD to check feasibility of the FIT process (8). The target capacity was 100,000 t/y of iron. Two types of reactors were designed in this step of reactor development such as (a) reactor producing metallic iron in solid state with an operating temperature of 1300°C (b) reactor producing iron in the molten state with an operating temperature of 1600°C (6). Different types of burner designs and different diameters were investigated in this CFD work (as shown in Figure 32). For one burner configuration, reactors with 6 m diameter showed better particle and temperature distributions than that of 4 m diameter reactors. Also, there was less heat loss for reactors with a diameter of 6 m. A reactor with a diameter of 6 m and 4 burners was also simulated. The larger numbers of burners ensure better particle distribution and lower probability of particle sticking. It was argued that though CFD results may vary quantitatively from the real case, it was able to show how design variation can affect the process parameters to a great extent (8).

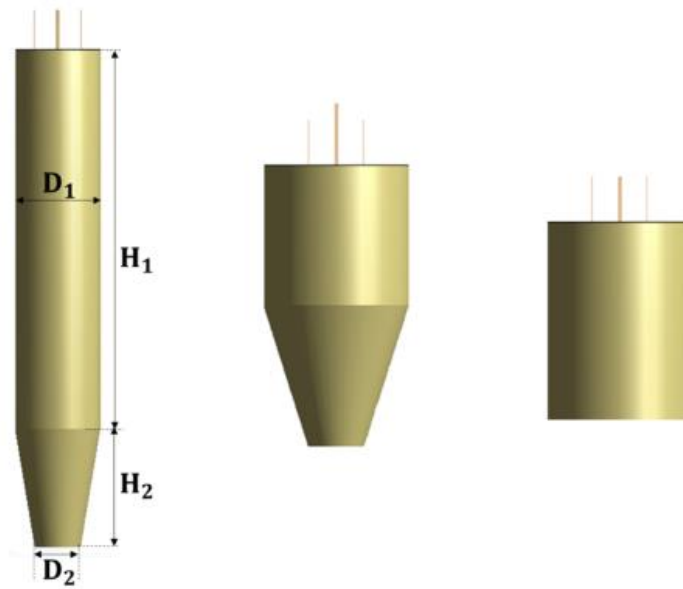


Figure 32 Different configuration of FIT reactor (8)

5.3.4 Design of Industrial Flash Ironmaking Reactors

An industrial flash ironmaking plant should be operating with the capacity of at least 0.3 to 1.0 million t/y of iron to be competitive with blast furnaces, which have the capacity of 0.3 to 3.0 million t/y of iron. Though multiple burners in the reactors were proven to be more effective, single burners with four feeding ports were designed into these industrial reactors to reduce computational times and challenges (8). Two reactors with the capacity of 0.3 million t/yr of iron and 3 million t/yr of iron were simulated (as shown in Table 9) using CFD modelling technique.

Table 9 Industrial Flash Ironmaking Reactors (8)

Parameter	Reactor 1	Reactor 2
Target production of iron in million t/y.	0.3	1.0
Feed of the magnetite concentrate in million t/y.	0.415	1.38
Natural gas feeding rate in m ³ /s	17.5	45.8
Oxygen feeding rate in m ³ /s	13.2	34.7
Expected excess of hydrogen at full reduction (EDF)	0.3	0.3

Table 10 shows the gas composition and metallization rate at the reactor outlets. In Reactor 2, there was a higher outlet gas temperature, uniform temperature distribution, better particle distribution with less chance particles sticking on the wall and lower percentage of heat loss compared to reactor 1.

Table 10 Gas composition and metallization rate at the reactor outlets (8)

Reactor	T (K)	H ₂	CO	CO ₂	H ₂ O	Metallization (%)
1	1519	40.2	26.3	5.9	24.1	91.2
2	1578	39.9	26.6	5.7	24.8	91.4

The latest CFD work of flash ironmaking technology (FIT) (8) showed that the process has the same production scale as that of the blast furnace. The height of the furnace can be reduced using multiple burners and preheating the feed gas. The total volume of the reactor can be decreased by using increased pressure which also has downside of increasing cost due to safety concern. CFD results also indicated that working in larger diameter to height ratio is preferable due to lower heat loss. Multiple burners may need to be added in such conditions. The research is ongoing and there is still scope of incorporating the findings into the industrial flash ironmaking process and optimize its furnace design (8).

5.4 Fluidised Bed Processes

In fluidised bed technology, fine ore can be directly reduced without sintering or pelletizing which optimises the cost of the ironmaking processes (10) FINMET, Circored, FINEX and Hismelt are the name of the processes that utilise fluidised bed technology (11) Hismelt and FINEX both produce liquid iron from a melting/smelting stage after reduction in a fluidised bed(s). The latest development of Primetals technologies – HYFOR (11) process have similarities with FINMET and Circored process as it uses direct reduction processes using H₂-rich gas or 100% H₂ as the reducing gas with iron ore fines.

5.4.1 FINMET

The FINMET process uses natural gas which is reformed with steam to produce the reducing gas. The iron ore fines go through the four-stage fluidised bed system and reached 800°C at the final bed. The reducing gas enters the bed system in counter flow arrangement (as shown in Figure 8). As the ore fines passed through the beds by gravity, it is gradually reduced by the reducing gas. At the end, the highly metallised DRI fines are hot compacted to HBI (10).

5.4.2 Circored

Circored is the only H₂ based process that has operated at commercial scale. In this process, H₂ is used as the reducing gas. The iron ore fines are first dried and then pre-heated in a circulating fluidised bed preheater (as shown in Figure 9). Then it goes to the circulating fluidised bed reactor. After being pre-reduced, the iron ore fines go to the bubbling fluidised bed reactor for the final reduction where cross flow of ore fines and reducing gas takes place. The temperature at the last reactor reaches about 630 to 650°C. It is then discharged to flash heater where DRI fines are heated for hot briquetting (10).

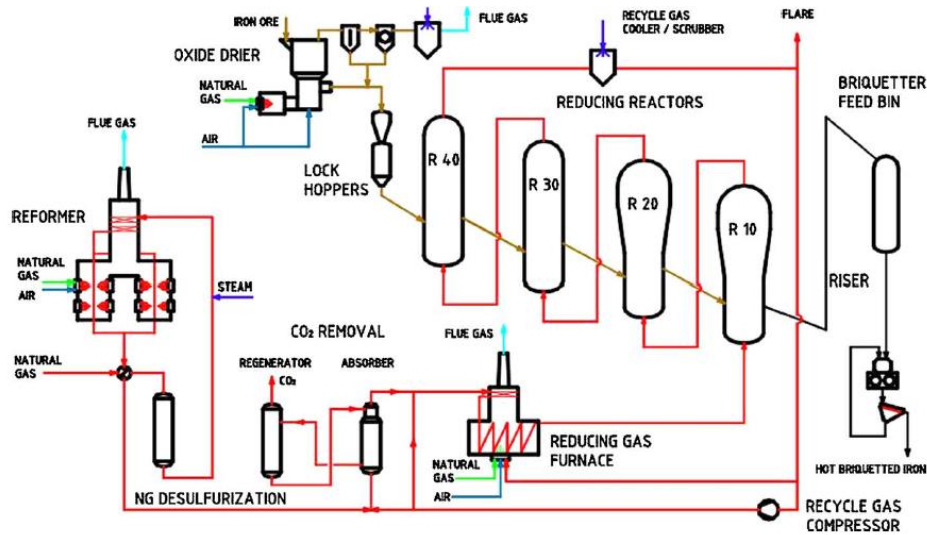


Figure 33 FINMET Process (10) (12)

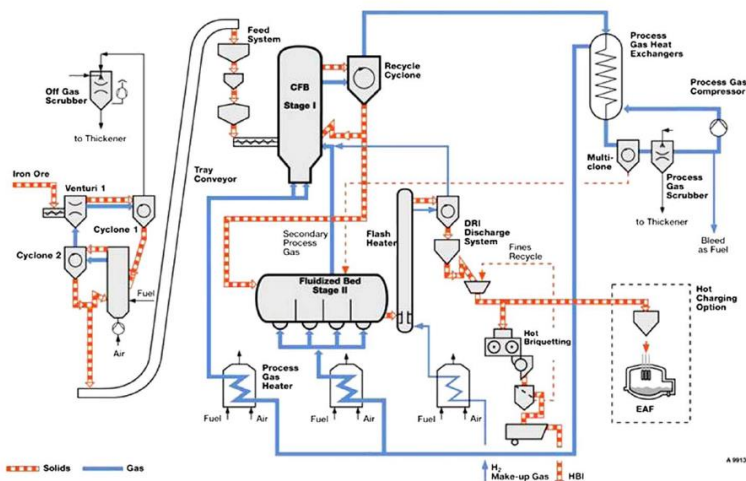


Figure 34 Circored Process (10) (13)

In the FINEX process, there are four fluidised bed reactors and a melter gasifier (as shown in Figure 35). First, dried iron ore fines are charged into the four fluidised bed reactors with fluxes like limestone. As iron ore fines are moved from the series of bed reactors, they are heated and reduced to DRI by hot reducing gas. This gas has been produced from the gasification of coal. Then DRI fines are hot compacted to HBI. It is then sent to melter gasifier to convert into hot metal (10).

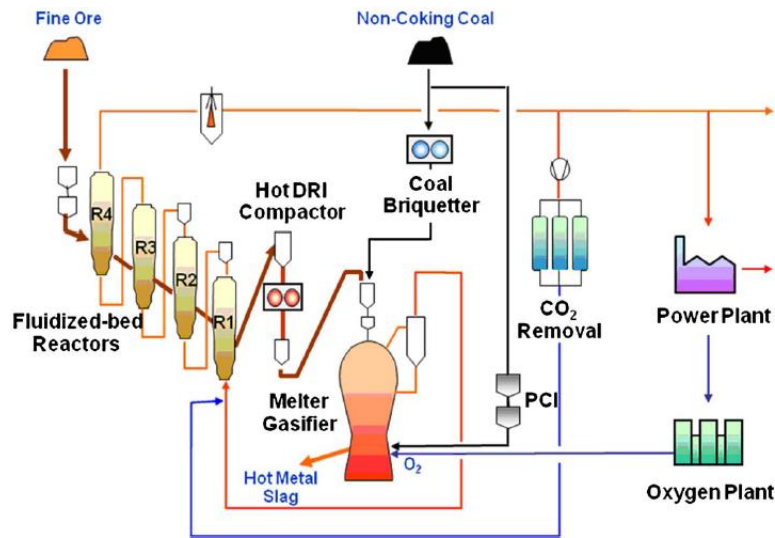


Figure 35 FINEX Process (10) (14)

5.4.3 Hismelt

The Hismelt is a smelting reduction process based on the gasification of coal with oxygen enriched hot air. As shown in Figure 11, the iron ore fines are preheated by the circoheat system of Metso (formerly Outotec) using a part of hot gas from the smelter. This system consists of circulating fluidised bed with two stages of cyclones. It is used to pre-reduce the iron ore to magnetite/wustite (10). This ore preheater with Hismelt SRV flow sheet is most common option. There are other options such as Circofer with Hismelt SRV and Rotary hearth with Hismelt SRV. It has been claimed that Hismelt will have the likelihood of having lower cost and will be more environmentally friendly than that of BF (15).

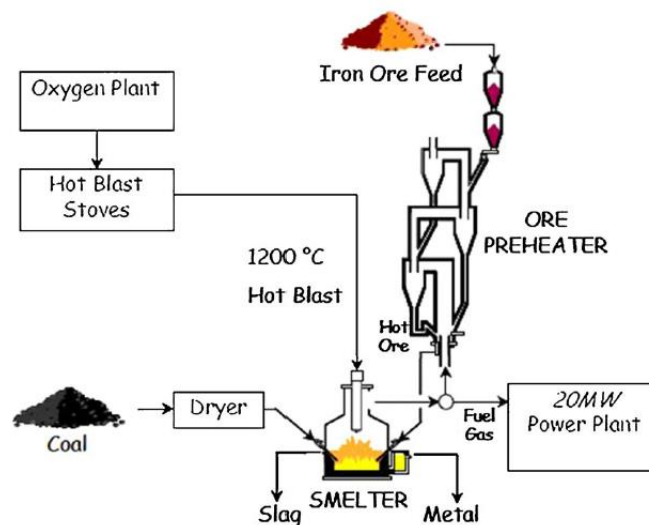


Figure 36 Hismelt process (10) (16)

5.4.4 HYFOR – Hydrogen-based Fine-Ore Reduction

In the HYFOR process, iron ore concentrates with particle size of less than $150\ \mu\text{m}$ can be used. Without any agglomeration, different types of ores such as hematite, limonite, magnetite can be reduced in this process. It has cross current flow of the reducing gas and iron ore concentrates (as shown in Figure 37). H_2 is used as the reducing agent. Low temperature, typical of fluidised bed technology, can be used to reduce the iron ore concentrates (17).

The concentrates are preheated to reach the desired temperature before reduction happens. For magnetite ores due to its poor reducibility, there is provision for an additional oxidation reaction taking place during material pre-heating. After preheating, the iron ore concentrates are charged from material bins to the HYFOR reactor. The reactor has a cross section of less than $1\ \text{m}^2$. The material enters the reactor on one side, while on the other side, a weir is installed to ensure a definite bed height. Thus, the residence time can be adjusted. Materials passing the weir can be transported back pneumatically and can be charged again to attain the desired metallization. H_2 is also preheated before entering the reactor. After reducing to the set metallization rate, DRI concentrates are collected again in the material bins and discharged into a quenching vessel (17). The next step of HYFOR is an industrial prototype plant with a production capacity of approximately 5-15 tons per hour considering continuous operation. A proposed schematic flow diagram of a HYFOR industrial prototype plant is shown in Figure 38 is expected to be operational by 2025.

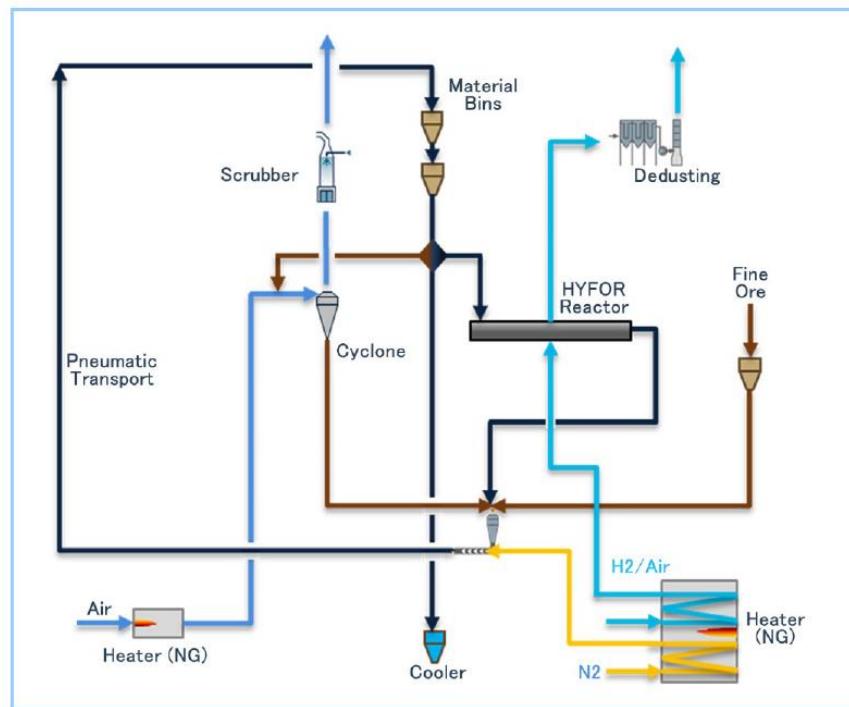


Figure 37 HYFOR Pilot plant (17)

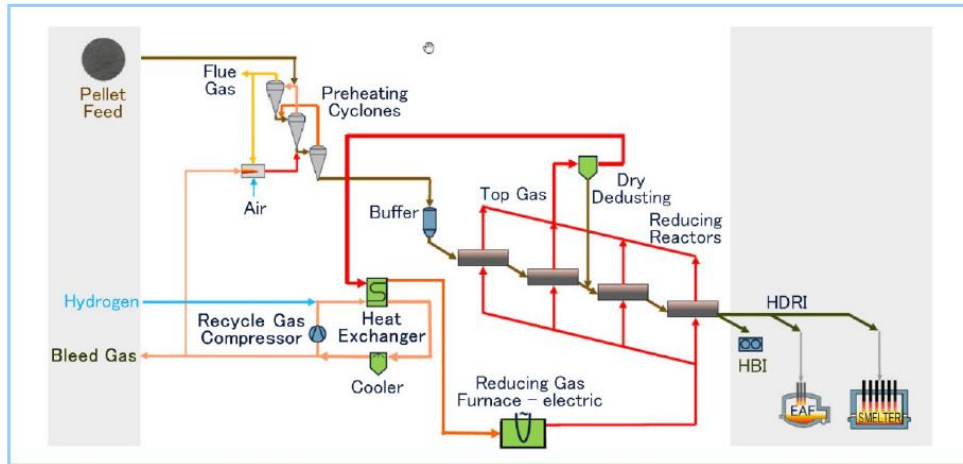


Figure 38 HYFOR Industrial prototype plant (17)

5.4.5 Hydrogen reduction – HyREX

The South Korean company, POSCO is developing a hydrogen-based ironmaking demonstration plant called HyREX in collaboration with Primetals Technologies. 30 years of experience in R&D, and a commercialization experience of 250Mt FINEX in its process, HyREX is expected to be great addition to other hydrogen ironmaking technologies (18). The HyREX process is composed of multi-stage fluidised bed reactors connected in series (as shown in Figure 14). For the downstream processes, two pathways are considered. One pathway includes melting of DRI with scrap in an EAF followed by secondary refining and continuous casting. The other pathway is to smelt DRI with carbon loaded in an electric smelting furnace (ESF) to produce the hot metal. Then the hot metal is processed by BOF followed secondary refining and continuous casting (18). POSCO is planning to build a test facility by 2028 to assess the commercial feasibility of HyREX. It is also starting demonstration phase from 2025 without any pilot phase and verify the technology by 2030 (19).

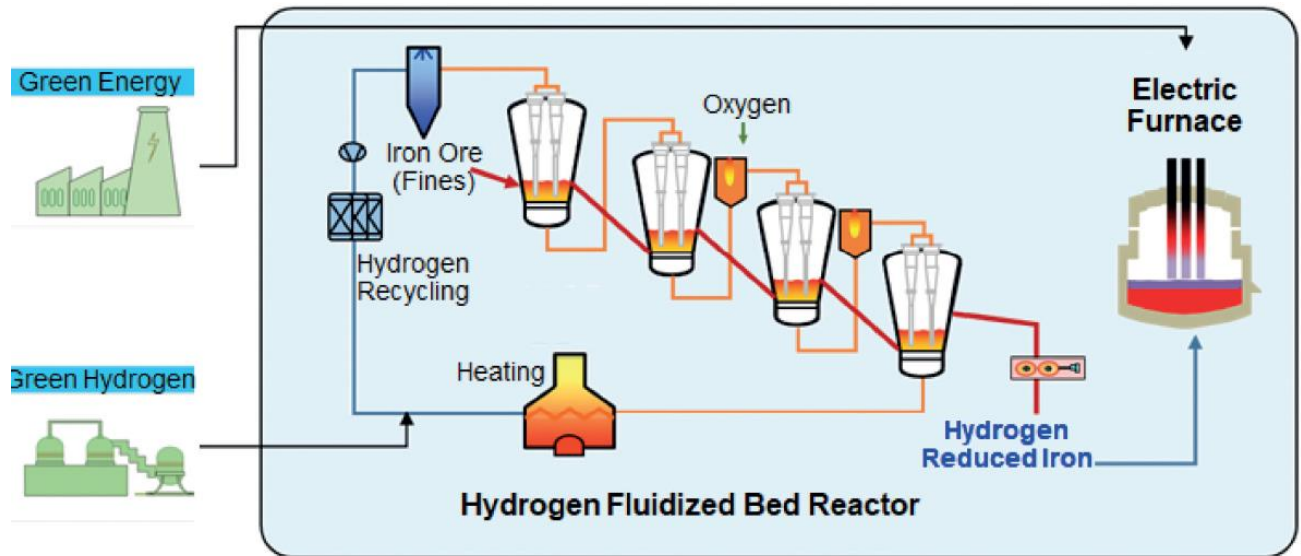


Figure 39 HyREX process flowsheet (18)

5.5 Comparison Between the Technologies

5.5.1 Characteristics of The Process

The technologies that are most comparable to ZESTY are Flash Ironmaking Technology (FIT)- H₂, Fluidised Bed (FINMET) and Fluidised Bed (H₂)- HYFOR. Midrex (NG), and Midrex (H₂) have been included in the competitive technologies assessment as standards as well as its well-known competitive position among direct reduction technologies.

Almost all the complete technologies, except HYFOR, have counter flow arrangements. HYFOR has cross current flow arrangement. Residence time wise, Midrex is the slowest process (pellets spend hours in the shaft) whereas FIT has the shortest reduction time (in the order of seconds). Most of the competitive technologies work at atmospheric pressure except for FINMET. It works at the most highest-pressure condition (i.e., 11 to 14 bar). Feed material of HYFOR, FINMET, FIT and ZESTY are quite similar though particle size varies to some extent. While Midrex, HYFOR, FINMET and ZESTY work below 1000 °C, FIT process works at higher temperature (i.e., 1200 to 1600 °C). Table 11 below summarises the various different characteristics of the processes.

Table 11 Comparison between the technologies based on characteristics of the process.

Name of the Technology	ZESTY	Flash Ironmaking Technology (FIT) - Sohn process (H ₂)	Midrex (NG)	Midrex (H ₂)	Fluidised Bed (FINMET)	Fluidised Bed (H ₂)-HYFOR
Type of reduction	DR	DR	DR	DR	DR	DR
Number of steps	1 step	1 step 2 steps	1 step	1 step	4 stages	4 stages
Description of the reactor	multiple number of tubes	one reactor (1 step) one ironmaking reactor and one prerduction reactor (2 steps)	Shaft furnace	Shaft furnace	Four fluidised beds	Four fluidised beds
Feed material	Iron ore fines	Iron ore concentrates	Iron ore pellets (80%) and lump ore (20%)	Iron ore pellets (80%) and lump ore (20%)	Iron ore fines	Iron ore concentrates

Feed rate	60 kg/h (semi-continuous mode)	1 to 7 kg/h (pilot flash reactor) (8)	1.42 tons/t DRI (for 1 Mtpa DRI plant) (20)	1.42 tons/t DRI (for 1 Mtpa DRI plant) (20)	-	-
Particle size	38 to 130 μm (1)	20 to 53 μm (21)	Pellets (95%) - 9 to 16 mm, lump (85%) -10 to 35 mm (22)	Pellets (95%) - 9 to 16 mm, lump (85%) -10 to 35 mm (22)	<12 mm (23)	<150 μm (17)
Reducing gas	Hydrogen	Hydrogen	Natural gas	Hydrogen	Natural gas	Hydrogen
Gas rate	9 to 13.5 Nm ³ /t DRI at Pilot plant	0.9 Nm ³ /hr to 3.6 Nm ³ /hr (i.e., 15 to 60 LPM) at Pilot flash reactor (8)	1622 Nm ³ / t DRI to 2045 Nm ³ /t DRI (24)	550 Nm ³ /t DRI (as reductant) 250 Nm ³ /t DRI (as heat source) (23)	360 Nm ³ /t HBI (25)	550 to 600 Nm ³ / t DRI (estimated for pilot plant) (17)
Working temperature	950 °C (1)	1200 to 1600 °C (8)	750 to 1000°C (25)	750 to 1000°C (25)	350 to 850 °C (10)	950 °C (17)
Pressure	atmospheric	atmospheric	≤ 1 bar	≤ 1 bar	11 to 14 bar	
Residence time	order of 60 s (1)	10 to 19 seconds (8)	>360 mins	>360 mins	-	-
Arrangement of flow	counter current	concurrent	Counter current	Counter current	Counter current	cross current (17)

5.5.2 Techno-economic Comparison

Table 12 Comparison between the technologies based on techno-economics of the process.

Name of the Technology	ZESTY	Flash Ironmaking Technology (FIT) - Sohn process (H ₂)	Midrex (NG)	Midrex (H ₂)	Fluidised Bed (FINMET)	Fluidised Bed (H ₂)-HYFOR
CAPEX	Under development as Part of FEED	1 step process- AU\$ 651 million (1 million tons/yr capacity) 2 step process - AU\$ 1042 million (1 million tons/yr capacity)	AU\$ 477/ t DRI (23) AU\$ 593/ t without pelletizing cost, AU\$ 845 /t including pelletizing cost (HILT CRC project 1.004 & 1.005)	AU\$ 477/ t DRI (23) AU\$ 593/ t without pelletizing cost, AU\$ 845 /t including pelletizing cost (HILT CRC project 1.004 & 1.005)	AU\$ 400/t DRI (23) AU\$ 662/ t DRI (HILT CRC project 1.004 & 1.005)	AU\$ 662/ t DRI (Estimated from HILT CRC project 1.004 & 1.005)
OPEX	Under development as Part of FEED	1 step process- AU\$ 1257/ ton of hot metal 2 step process - AU\$ 1190/ ton of hot metal- H ₂ price AU\$6/kg)	AU\$ 566/ t DRI (20)	AU\$ 855/ t DRI (23)-depends on cost of H ₂ or electricity. AU\$ 392/t DRI (without pelletizing), AU\$ 605/t DRI (with pelletizing cost), H ₂ price AU\$6/kg) (HILT CRC project 1.004 & 1.005)	AU\$ 285/ t DRI (23)	AU\$ 329 / t DRI - H ₂ price AU\$6/kg (Estimated from HILT CRC project 1.004 & 1.005)

5.5.3 Technological Readiness Level

Among all the competitive technologies of ZESTY, FINMET is the most advanced in its TRL level. It has been placed at TRL level 9 since the technology is currently working as an Industrial plant in Puerto Ordaz, Venezuela after being closed for some time due to operational issues. Some challenges in the process include the requirement of high pressure, increased consumption of natural gas, lower production efficiency and agglomeration of ore particles . Though it has higher TRL level, the technology has not been widely commercialized like other ironmaking technologies. For Midrex (NG) and Midrex (H2), TRL is reported to be between 6 to 8 and 5 to 7 by IEA (26). It indicates there is still scope of widespread commercial application. Flash Ironmaking Technology (FIT), initially well supported by American Iron and Steel Institute, has is in TRL level 4 to 5. Unfortunately, FIT has not been developed beyond its pilot plant test at the university of Utah yet. ZESTY and HYFOR are both placed at the same TRL level. It is placed at TRL level 5 to 6 as both are going through pilot level tests and validations. ZESTY is currently testing its ability of process different types of iron ores whereas HYFOR is testing the process for various ore grades to generate relevant process data that can be used for scaling up to an Industrial prototype.

Table 13 Comparison between the technologies based on TRL level.

Name of the Technology	ZESTY	Flash Ironmaking Technology (FIT) Sohn process	Midrex (NG)	Midrex (H ₂)	Fluidised Bed (FINMET)	Fluidised Bed (H ₂)-HYFOR
Current Technological Readiness Level (TRL)	TRL 5 to 6	TRL 4 to 5	TRL 6-8 TRL 5 to 7 (IEA) (26)	TRL 6-8, TRL 5 to 7 (IEA) (26)	TRL 9	TRL 5 to 6

6 EMISSIONS REDUCTION POTENTIAL

Among the competitive technologies, the conventional BF-BOF route has the lowest carbon reduction potential. Though numerous investigations (27) (28) (29) (30) have been made to reduce the emissions of the existing Blast Furnace (BF) using waste plastic, biomass, injection of H₂ or hydrogen rich fuels, the reduction potential is estimated to be between 20% to 30% (31) which is low compared to other H₂ based technologies.

The next in line is FINMET- EAF route which has the reduction potential between 34% to 41%. It is important to mention that the CO₂ emission from EAF has been taken as 150 to 300 kg CO₂/tIs as reported in literature.

CO₂ emission in MIDREX varies depending on the percentage of natural gas and H₂ used in the process. For 100% NG, the emission is reported to be 500 kg CO₂/tDRI . In terms of reduction potential, our calculation shows that MIDREX (100% NG)-EAF route has the reduction potential between 59% to 67% which is similar to the value reported by MIDREX (20). MIDREX(H₂) has reported its CO₂ emission to be 193 kgCO₂/tDRI (20) where green H₂ has been used as the reductant and NG as the heating source. Thus, the CO₂ reduction potential via MIDREX-EAF route is estimated to be between 75% to 82% which is similar to the values reported in literature (32). It is reasonable to predict that with H₂ as the heating source, the reduction potential for MIDREX (H₂) will increase and would likely to be similar to ZESTY and other H₂ based technologies.

Without specifying any number, HYFOR has claimed that it can reduce to CO₂ emission close to zero. FIT estimated that 96% reduction of emission compared to Blast furnace operation (5). Mass and Energy balance model of ZESTY showed that with green H₂, its emission is close to zero. From our calculations, ZESTY-EAF, HYFOR-EAF and FIT-EAF show the greatest promise in terms of highest CO₂ reduction potential as high as 92%. The CO₂ output from ZESTY-EAF could increase if the DRI produced was carbonised using CO gas (as a means to assist in melting/refining in an EAF or Melter) and in this case, the CO₂ output would likely to be similar to the MIDREX(H₂)-EAF case.

Table 14 Comparison between the technologies based on CO2 emission.

Name of the Technology	ZESTY	Flash Ironmaking Technology (FIT) -H ₂	MIDREX (NG)	MIDREX (H ₂)	Fluidised Bed (FINMET)	Fluidised Bed (H ₂)- HYFOR
CO ₂ Emission	Close to zero	56 kgCO ₂ /t DRI (5)	500 kgCO ₂ /tDRI (100% NG) 400 kgCO ₂ /tDRI (80% NG) 250 kgCO ₂ /tDRI (50% NG) 150 kgCO ₂ /tDRI (30% NG)	193 kgCO ₂ /tDRI (20)	993 kg CO ₂ /t DRI/HBI (25)	Close to zero (11)

Table 15 Comparison between the technologies based on CO2 reduction potential.

Name of the Technology	BF-BOF	ZESTY – EAF	FIT- EAF	MIDREX (NG)- EAF	MIDREX (H ₂)-EAF	FINMET- EAF	HYFOR-EAF
CO ₂ Emission	1943 kg CO ₂ /t (20)	150 to 300 kgCO ₂ /t	206 to 356 kgCO ₂ /t	650 to 800 kgCO ₂ /t (100% NG)	343 to 493 kgCO ₂ /t	1143 to 1293 kgCO ₂ /t	150 to 300 kgCO ₂ /t
CO ₂ reduction potential	20% to 30% (31)	85% to 92%	82% to 89%	59% to 67%	75% to 82%	34% to 41%	85% to 92%

7 SITE SELECTION CONCLUSIONS

The decision to build a hydrogen-based iron ore reduction demonstration plant in Australia would depend on several factors, such as the availability of raw materials, labour force, energy costs, proximity to customers, government incentives, and availability of hydrogen-hub & electricity infrastructure.

The intention by this stage of the project was to have narrowed the site choice down, however further work is ongoing to fully understand the costs associated with each site, so as to allow commercial decisions relating to the demonstrator to take place.

Based on these general considerations, here are five potential sites that could be considered for building a demonstration plant in Australia:

1. **Port Augusta/Whyalla, South Australia:** Whyalla is already home to an iron and steelmaking plant, and its location near major iron ore deposits in the Middleback Ranges of South Australia makes it an ideal location for a demonstration plant.
2. **Kwinana, Western Australia:** Kwinana has an existing heavy industry sector, with access to raw materials such as iron ore and electricity. It is also well connected to transportation infrastructure and has a skilled labour force.
3. **Port Hedland, Western Australia:** Pilbara region is known for its rich iron ore deposits and a major source of iron ore exports to China and other Asian markets, which makes it an attractive location for a demonstration plant due to the availability of raw materials, a well-developed infrastructure and transportation network, including a deepwater port and rail connections. The town has access to a skilled labour force, and WA government has identified the Port Hedland as a priority area for investment and economic development for green steel and hydrogen projects.
4. **Gladstone, Queensland:** Gladstone has an established heavy industry sector and access to iron ore, hydrogen, and renewable electricity. It also has a deepwater port and is well connected to transportation infrastructure.
5. **Port Kembla, New South Wales:** Port Kembla is located near major iron ore deposits and has an existing steelmaking industry. It also has a deepwater port and is well connected to transportation infrastructure.

Table 16 outlines the plant site selection criteria for ZESTY Demo Plant H-DRI 30,000 TPA, with the top three preferred site locations at:

1. **Port Hedland, Western Australia**
2. **Port Augusta/Whyalla, South Australia**
3. **Port Kembla, New South Wales**

7.1 Site Selection Executive Summary

Australia's shift towards green hydrogen production for steelmaking presents opportunities, especially given its abundant renewable energy and iron ore reserves. However, challenges like high electrolysis costs, lack of hydrogen infrastructure, and the need for technological innovation persist.

The study identified areas in Australia with high potential for green steel production, with a significant focus on the Pilbara and South Australia regions. The Pilbara region, in particular, is rich in high-grade hematite-goethite mix ores, while South Australia has a substantial magnetite-rich resource base, but with enough haematite resources for the demonstration plant.

Among the four potential locations, Port Augusta stands out as the most strategic choice for green hydrogen production, closely followed by Port Hedland, Whyalla, and then Port Kembla. Port Augusta's abundant renewable energy resources, proximity to iron ore mines, and existing infrastructure make it a prime candidate. Port Hedland's significant industrial infrastructure and solar energy potential place it as a close second. Whyalla's historical significance in steelworks and shipbuilding, combined with its renewable energy potential, ranks it third. Lastly, Port Kembla, with its proximity to Sydney and potential for wind energy, rounds out the list. While each location has its unique advantages, Port Augusta's combination of factors provides a compelling case for its selection.

Whyalla: Whyalla boasts a rich history in steelworks and shipbuilding. The city's historically low electricity prices are attributed to the integration of renewable energy. With an exceptional wind resource and potential for solar energy, Whyalla presents a strong case. Land is available at reasonable prices, but the limited freshwater resources might necessitate water treatment processes. The established rail and port facilities can be advantageous for material transport. However, fluctuating electricity prices and water scarcity pose challenges.

- **Location:** Situated in South Australia, Whyalla is historically known for its steelworks and shipbuilding.
- **Electricity:** Historically, Whyalla has enjoyed low electricity prices, which can be attributed to the integration of renewable energy sources.
- **Renewable Energy:** Whyalla boasts an exceptional wind resource, making it a prime location for harnessing wind energy. Additionally, there's potential for solar energy utilisation.
- **Land and Water:** Land is available at reasonable costs, which can be advantageous for setting up the plant. The limited freshwater resources mean that water treatment processes might be necessary.
- **Infrastructure:** The city has established infrastructure, including steel, rail and port facilities, which can be leveraged for transporting materials and finished products.

Port Kembla: Port Kembla, an industrial hub in New South Wales, is strategically positioned near Sydney, leading to higher electricity demand and prices. The region's potential for wind energy and its coastal location for seawater access are notable strengths. However, desalination would be required, and economic considerations include higher labour costs. The established industrial base is a strength, but the higher operational costs might be a deterrent.

- **Location:** Located in New South Wales, Port Kembla is an industrial hub.
- **Electricity:** Proximity to Sydney means there's a higher electricity demand, results in higher electricity prices compared to Whyalla.
- **Renewable Energy:** The region has potential for wind energy utilisation.
- **Water:** The location offers access to vast amounts of seawater, and probability tap water.
- **Economic Factors:** Labor costs in Port Kembla are higher than in Whyalla, which can influence the overall cost of setting up and operating the plant.

Port Hedland: Port Hedland is a significant mining and export hub. The region is abundant in solar energy potential, but wind energy faces challenges due to suboptimal conditions and turbine size limitations. The coastal town provides access to seawater, but direct utilisation in electrolyzers is still under development, and traditional methods might involve desalination. The tropical weather, with its recurring cyclones, poses infrastructure and operational challenges. However, the town's substantial industrial infrastructure and the proximity to the iron ore mines is a significant advantage.

- **Location:** Port Hedland, situated in the Pilbara region of Western Australia, is predominantly known for its mining activities, especially iron ore.
- **Infrastructure:** Given its significance as an export hub, Port Hedland has substantial industrial infrastructure, which can be advantageous for setting up the plant.
- **Renewable Energy:** The Pilbara region is rich in solar energy potential, which can complement the electrolyser plant. However, the region faces challenges with wind energy due to suboptimal conditions and limitations on wind turbine sizes.
- **Water:** As a coastal town, Port Hedland has abundant access to seawater. However, using tap water is challenging due to the prevalent water scarcity.
- **Environmental Factors:** The tropical weather in northwestern Australia means the region faces a recurring cyclone problem, which can impact infrastructure and operations.

Port Augusta: Port Augusta is at the forefront of the state's renewable energy transition. The region supports various solar and wind projects and is strategically located near iron ore mines in the Eyre Peninsula. Existing infrastructure, including rail and port facilities, coupled with grid expansion plans, enhances its attractiveness. Land is abundant and reasonably priced. Engaging with local Aboriginal communities, such as the Barngarla people, is crucial. The potential impacts on the port's historic and aesthetic values also need consideration. Overall, its strategic importance and abundant resources make it a top contender.

- **Location:** Port Augusta, located in South Australia, is strategically positioned and plays a pivotal role in the state's renewable energy adoption.
- **Renewable Energy:** The region supports various solar and wind projects, providing access to abundant renewable energy resources. The proximity to iron ore mines in the Eyre Peninsula region further enhances its strategic importance.
- **Infrastructure:** Existing infrastructure, including rail and port facilities, can be leveraged for the project. Additionally, there are grid expansion plans in place to support the integration of more renewable energy sources.
- **Economic Factors:** Land availability in Port Augusta is substantial, with costs being generally moderate. The strategic location might make it an attractive option for industries.

- Community and Cultural Factors:** There's a need to respect and engage with local Aboriginal communities, such as the Barngarla people. Additionally, potential impacts on the historic and aesthetic values of the port and its surroundings need to be considered.

Table 16 Comparative Table of Advantages and Disadvantages

Location	Advantages	Challenges
Whyalla	<ul style="list-style-type: none"> - Historically low electricity prices - Exceptional wind resource - Established infrastructure - Proximity to iron ore mines 	<ul style="list-style-type: none"> - Limited freshwater resources - Fluctuating electricity price
Port Kembla	<ul style="list-style-type: none"> - Potential for wind energy - Potential collaboration with BlueScope - Existing infrastructure 	<ul style="list-style-type: none"> - Higher electricity and labour costs - High land price - Community engagement - Densely Populated area with limited available land
Port Hedland	<ul style="list-style-type: none"> - Rich in solar energy potential - Significant industrial infrastructure - Proximity to iron ore mines 	<ul style="list-style-type: none"> - Suboptimal conditions for wind energy - Recurring cyclones - Water scarcity issues
Port Augusta	<ul style="list-style-type: none"> - Abundant renewable energy resources - Proximity to iron ore mines - Shared Infrastructure - Strategic location for green steel and hydrogen export 	<ul style="list-style-type: none"> - Need to engage with local Aboriginal communities

7.2 Technology and Types of Electrolysers Summary:

The emission reduction potential and economics of green steel plant, either a demonstrator or commercial scale, depends heavily on the source of hydrogen. Continued work has been undertaken to characterise the opportunities and costs associated with different electrolyser solution.

The electrochemical decomposition of water into hydrogen and oxygen involves two electrodes in an electrolyte connected to a direct current (DC) supply. When a sufficient voltage is applied, hydrogen is produced at the cathode and oxygen at the anode. A separator ensures the gases don't mix while allowing ion transport.

There are three primary types of electrolysers:

1. Alkaline Electrolysers:

- Use a liquid electrolyte, typically potassium hydroxide (KOH).
- Mature technology with over 100 years of history.
- Advantages: Low capital costs, high durability, and scalability.

- Drawbacks: Low efficiency, slow response, sensitivity to water impurities, and the need for corrosive chemicals.

2. PEM Electrolysers:

- Use a solid polymer membrane as the electrolyte.
- Advantages: Higher efficiency, faster response, lower sensitivity to impurities, and can operate at higher pressures and temperatures.
- Drawbacks: High capital costs, lower durability than alkaline, and limited scalability.

3. Solid Oxide Electrolysers:

- Use a ceramic material as the electrolyte.
- Operate at high temperatures (~800°C), making them highly efficient.
- Can use other fuels like CO₂ or methane to produce syngas or synthetic fuels.
- Challenges: High capital costs, low durability, long start-up time, and high thermal stress.

Suitability for a H₂-DRI production

- **Alkaline electrolysers** are ideal for large-scale production with stable electricity and low-cost water sources. They can be integrated with renewables but might need backup power (29).
- **PEM electrolysers** are suitable for small-scale or distributed production with variable electricity and high-quality water sources. They can quickly adapt to electricity supply changes.
- **Solid oxide electrolysers** are best for using waste heat or solar thermal energy and co-producing synthetic fuels. They can be integrated with high-temperature heat sources but have long start-up times.

Reason for Choosing Alkaline Electrolysers: The decision to opt for alkaline electrolysers is based on a few compelling reasons:

- **Maturity:** Alkaline electrolysers represent a time-tested technology with a history spanning over a century.
- **Economical:** They offer the most cost-effective capital cost when compared to alternatives like PEM.
- **Availability:** Their widespread presence ensures a shorter lead time for procurement and setup.
- **Risk Mitigation:** Using alkaline electrolysers is a strategic choice to reduce potential risks associated with newer or less established technologies.

The electrolyser footprint is relatively constant for alkaline electrolysers, while the utilities footprint increases with higher operating pressure. The total footprint ranges from about 60 to 70 m² per MW for alkaline electrolysers.

A study by GPA Engineering, commissioned by APGA, revealed that historically, pipelines have been more cost-effective and reliable than powerlines for energy transmission. The study considered various scenarios, including distances ranging from 25km to 500km and energy flows from 10 TJ/day to 500 TJ/day (30)

Findings indicated that hydrogen pipelines are up to three times more cost-effective than powerlines for similar distances and capacities. Storing energy in hydrogen pipelines is also significantly cheaper than in battery systems (BESS) or pumped hydro storage (PHES). For hydrogen consumers, these pipelines offer benefits beyond cost savings. Producing hydrogen closer to the energy source results in cheaper electrolysis energy. Consuming energy before its transport and storage can reduce hydrogen prices for consumers by around 30%.

For ZESTY, the takeaway is that generating hydrogen at the renewable energy source is more cost-effective than transmitting electricity to a site and then producing hydrogen. If using existing electricity infrastructure, a Power Purchase Agreement (PPA) is recommended, which may incur Transmission Use of System (TUOS) charges estimated at \$15-25/MWh.

The techno-economics and emissions reduction potential of any H2 DRI plant, including ZESTY, are heavily dependent on the levelised cost of green energy used to generate the H2. Due to this, further work is underway to fully capture the evolving H2 economy and to understand the best outcome for the ZESTY process, both at a demonstration level and for future scale up.

8 CONCLUSIONS AND NEXT STEPS

The pilot plant test work has been completed at Calix's Bacchus Marsh R&D facility allowing the learnings to feed into the sizing of the plant and further the understanding of where ZESTY can be used for green steel production.

The pilot plant test results showed good metallisation rates across a range of process conditions. Trends indicate that the process can be suited to a range of process conditions but with the limiting factor likely to be material recovery, particularly at higher gas flows and finer PSDs.

Further work will be undertaken to understand these trade-offs and optimise the system to understand the effect on CAPEX and OPEX efficiencies and inform the techno-economics.

The two selected Hematite/Goethite ores show consistent results with some performance differences potentially attributable to the difference in PSD. The key outcome is that the ZESTY process is potentially suitable for differing Hematite/Goethite ore bodies that make up the majority of Australia's Iron ore deposits.

This investigation will be continued with a wider range of ores provided through partnerships with HILT CRC participants and other commercial partners.

Emissions reduction and techno-economics have been developed further towards completion of the FEED study. This report includes summaries of comparisons between ZESTY and other technologies. As the FEED study continues further work will be done on the techno-economics and emissions reduction potential once all inputs are further understood.

9 REFERENCES

1. *Calix' Zero Emissions Steel Technology (ZESTY) – Flash Hydrogen Direct Reduction of Low-Grade Ores to Green Iron and Steel Products*. **M.E. Boot-Handford, T.D., B.A. Nuraeni, I. Rosa Ignacio, Y. Xia, A. Adipuri, M. Gill, A. Okely, P. Hodgson, M. Sceats, G.A. Brooks**. 2023, METEC & 6th ESTAD.
2. *CFD study of hydrogen injection in blast furnaces: tuyere co-injection of hydrogen and coa*. **Liu, Y., Z. Hu, and Y. Shen**. 2021, Metallurgical and Materials Transactions B, pp. 52(5): p. 2971-2991.
3. **Cavaliere, P.** *Hydrogen assisted direct reduction of iron oxides*. s.l. : Springer, 2022.
4. **McGregor, K.** [Online] 2018. <https://research.csiro.au/resourcesandsustainability/overcoming-inefficiencies-in-flash-smelting/>.
5. *Novel flash ironmaking technology with greatly reduced energy consumption and CO 2 emissions*. **Sohn, H.Y., M. Choi, and M. Olivas-Martinez**. 2012, 6th International Congress on the Science and Technology of Ironmaking.
6. *Development of a Novel Flash Ironmaking Technology with Greatly Reduced Energy Consumption and CO2 Emissions*. **Sohn, H.Y. and Y. Mohassab**. 2016, Journal of Sustainable Metallurgy, pp. 2(3): p. 216-227.
7. *Energy consumption and CO2 emissions in ironmaking and development of a novel flash technology*. **Sohn, H.Y.** 2019, Metals, p. 10(1): p. 54.
8. *Design of novel flash ironmaking reactors for greatly reduced energy consumption and CO2 emissions*. **Sohn, H.Y., D.-Q. Fan, and A. Abdelghany**. 2012, Metals, p. 11(2): p. 332.
9. *Steel industry and carbon dioxide emissions-a novel ironmaking process with greatly reduced carbon footprint*. **Sohn, H. and M. Choi**. 2012, Carbon dioxide emissions: new research, p. 11788.
10. *Recent status of bed technologies for producing iron input materials for steelmaking*. **Schenk, J.L.** 2011, Particuology, pp. 9(1): p. 14-23.
11. **Primetals**. [Online] 2021. <https://www.primetals.com/press-media/news/hyfor-pilot-plant-under-operation-the-next-step-for-carbon-free-hydrogen-based-direct-reduction-is-done..>
12. *bed applications for iron production*. **Peer, G. FINMET® and FINEX®**. 2005, IFSA.
13. *Operational results of the Circored fine ore direct reduction plant in Trinidad*. **Elmquist, S.** 2002, Stahl und Eisen, pp. 122(2): p. 59-64.
14. *From fine iron ore to hot metal*. **Schenk, J. FINEX®**. Linz, Austria : s.n., 2006. Proceedings of the innovations in ironmaking session of 2006 international symposium.
15. *Hlsmelt - Competitive Hot Metal from Ore Fines and Steel Plant Wastes*. **R J Dry, C.P.B.a.D.P.P.** 1999, Metec.

16. *Hismelt—the alternative ironmaking technology*. **Burke, P. and S. Gul**. 2002, In Proceedings of International Conference on Smelting Reduction for Ironmaking, Jouhari, AK, Galgali, RK, Misra, VN, Eds, pp. pp. 61-71.
17. **Daniel Spreitzer, J.W., Bernhard Hiebl, Norbert Rein, Thomas Wolfinger, Wolfgang Sterrer, Alexander Fleischanderl**. *HYFOR – HYdrogen-based Fine-Ore Reduction*. s.l. : Mitsubishi Heavy Industries Technical Review, 2022.
18. *Carbon neutrality: the industry's goal*. **Kim, K**. 2022, Steel Times International, pp. 54-57.
19. *POSCO's HyREX: cutting-edge green steel technology to watch out for*. **Rudra, T**. 2022.
20. *MIDREX H2 – The Road to CO2-free Direct Reduction*. **Robert Millner, J.R., Barbara Rammer, Christian Boehm, Wolfgang Sterrer, Hanspeter Ofner, Vincent Chevrier**.
21. *Hydrogen reduction kinetics of magnetite concentrate particles relevant to a novel flash ironmaking process*. **Wang, H. and H. Sohn**. 2013, Metallurgical and Materials Transactions B, pp. 132-145.
22. **Satyendra**. *Midrex Process for Direct Reduction of Iron Ore*. 2017.
23. *Decarbonisation and hydrogen integration of steel industries: Recent development, challenges and technoeconomic analysis*. **Shahabuddin, M., G. Brooks, and M.A. Rhamdhani**. 2023, Journal of Cleaner Production, p. 136391.
24. *Detailed modeling of the direct reduction of iron ore in a shaft furnace*. **Hamadeh, H., O. Mirgaux, and F. Patisson**. 2018, Materials, p. 11(10): p. 1865.
25. *CO2 abatement in the iron and steel industry*. **Carpenter, A**. 2012, IEA Clean Coal Centre, p. 25: p. 193.
26. *Technology Assessment and Roadmapping (Deliverable 1.2)*. **Draxler, M., et al**. 2021, Green Steel for Europe Consortium.
27. *Effect of H2 on blast furnace ironmaking: A review*. **Lan, C., et al**. 2022, Metals, p. 12(11): p. 1864.
28. *Review of hydrogen-rich ironmaking technology in blast furnace*. *Ironmaking & Steelmaking*. **Chen, Y. and H. Zuo**. 2021, pp. 48(6): p. 749-768.
29. *Fundamental experiments on the H2 gas injection into the lower part of a blast furnace shaft*. **Usui, T., et al**. 2002, ISIJ International, pp. 42(Suppl): p. S14-S18.
30. *Blast furnace hydrogen injection: Investigating impacts and feasibility with computational fluid dynamics*. **Okosun, T., S. Nielson, and C. Zhou**. 2022, JOM, pp. 74(4): p. 1521-1532.
31. *Personal communication*. **Brooks, G.A**. 2023.
32. *Ultra-Low CO2 Ironmaking: Transitioning to the Hydrogen Economy*. **Chevrier, V.F**. 2020.
33. *Power-to-steel: reducing CO2 through the integration of renewable energy and hydrogen into the German steel industry*. **Otto, A., et al**. 2017, Energies, pp. 10(4), 451.

34. **Sohn, H.Y.** *Flash Ironmaking*. Boca Raton : s.n., 2023.
35. **Sohn, H.Y.** *Celebrating the Megascale: Proceedings of the Extraction and Processing Division Symposium on Pyrometallurgy in Honor of David GC Robertson*. s.l. : Springer, 2016.
36. *The production and application of hydrogen in steel industry*. **Liu, W., et al.** 2021, International Journal of Hydrogen Energy, pp. 46(17): p. 10548-10569.
37. *Potential CO₂ emission reduction for BF–BOF steelmaking based on optimised use of ferrous burden materials*. **Wang, C., C. Ryman, and J. Dahl.** 2009, International Journal of Greenhouse Gas Control, pp. 3(1): p. 29-38.
38. **Montague, S.** Direct From Midrex. [Online] 2021. <https://www.midrex.com/wp-content/uploads/Midrex-DFM-1stQtr2021-Final.pdf>.
39. *Decarbonisation-Two steps towards net zero carbon?* **Wimmer, G., J. Rosner, and A. Fleischander.** Linz, Austria : s.n., 2022, Primetals Technologies Austria GmbH.